

Development of $\text{ZrB}_2\text{-B}_4\text{C-Mo}$ ceramic matrix composite for high temperature applications

A thesis submitted in partial fulfilment of the requirements for the degree of

Master of Technology

in

Metallurgical and Materials Engineering

by

Rajan Vedant

(Roll No. 213MM1476)



**Department of metallurgical and materials engineering
National institute of technology Rourkela
Rourkela, Odisha-769008**

Development of $\text{ZrB}_2\text{-B}_4\text{C-Mo}$ ceramic matrix composite for high temperature applications

A thesis submitted in partial fulfillment of the requirements for the degree of

Master of Technology

In

Metallurgical and Materials Engineering

By

Rajan Vedant

*Under the guidance
of*

Prof. Swapan Kumar Karak



**Department of Metallurgical and Materials Engineering
National Institute Of Technology, Rourkela
Rourkela, Odisha-769008**



**Department of Metallurgical and Materials Engineering
National Institute of Technology Rourkela
Rourkela, Orissa-769008**

Certificate

This is to certify that the thesis entitled “**Development of $\text{ZrB}_2\text{-B}_4\text{C-Mo}$ ceramic matrix composite for high temperature applications**”, submitted to the National Institute of Technology, Rourkela by **Mr Rajan Vedant**, Roll No: **212MM1476** for the award of Master of Technology in Metallurgical and Materials Engineering, at the National Institute of Technology, Rourkela, is an authentic work carried out by him under supervision and guidance. The experimental work and analysis of results are original work of the student and have not been presented anywhere for the award of a degree to the best of our knowledge.

Date:

Prof. Swapan Kumar Karak
Dept. of Metallurgical and Materials Engineering
National Institute of Technology Rourkela- 769008



**Department of Metallurgical and Materials Engineering
National Institute of Technology Rourkela
Rourkela, Orissa-769008**

Declaration

I certify that

- a) The work contained in the thesis is original and has been done by myself under the general supervision of my supervisor.
- b) The work has not been submitted to any other Institute for any degree or diploma.
- c) I have followed the guidelines provided by the Institute in writing the thesis.
- d) Whenever I have used materials (experimental analysis, and text) from other sources, I have given due credit to them by citing them in the text of the thesis and giving their details in the references.
- e) Whenever I have quoted written materials from other sources, I have put them under quotation marks and given due credit to the sources by citing them and giving required details in the references.

Date:

Rajan Vedant

Acknowledgement

With deep regards and profound respect, I avail this opportunity to express my deep sense of gratitude and indebtedness to **Prof. Swapan Kumar Karak, Department of Metallurgical and Materials Engineering, NIT Rourkela**, for introducing the present research topic and for his inspiring guidance, constructive criticism and valuable suggestion throughout this research work. It would have not been possible for me to bring out this report without his help and constant encouragement.

I express my sincere gratefulness to Dr. S C Mishra, Head of the Department, Metallurgical and Materials Engineering, NIT Rourkela for giving me an opportunity to work on this project and allowing me the access to valuable facilities in the department.

My special thanks go to Prof. D Chaira, Prof. A Patra, Prof. S.K. Sahoo for providing facility and giving me the valuable suggestion to carry out this project and also all professors of this department. I am highly grateful to laboratory members of the Department of Metallurgical and Materials Engineering, NIT Rourkela, especially, Mr. U.K. Sahu, Mr. Pradhan, Mr. A. Pal, Mr. Shyamu Hembram, Mr. Rajesh Pattnaik and Mr. Kishore Tanty for their help during the execution of experiments.

Last but not the least I would like to thank Mr R.R.Rout ,N. Mohan, S. Sravan Kumar and Shashanka R, all my classmates and my dear friends Vikash, Salim, Lala, Pranab for their encouragement and understanding. Most importantly, none of this would have been possible without the love and patience of my family. My family, to whom this dissertation is dedicated, has been a constant source of love, concern, support and strength all these years. I would like to express my heart-felt gratitude to them.

R Vedant
rajanvedant@gmail.com

ABSTRACT: The present study deals with development of ceramic matrix composite containing the nominal compositions of three powders ZrB_2 (40 wt. %), B_4C (40 wt. %) and Mo (20 wt. %) were synthesized by ball milling and followed by conventional sintering in a furnace at 1500°C and 1600°C for 3 hours in presence of Ar gas and also spark plasma sintering at 1800°C for 1 min. During ball milling the crystallite size of the powder gradually decreases with increase in milling time from 0h to 60h and crystallite size of the final product reaches in submicron or nano-metric level. The influence of the processing parameters on the phase evolution and chemical composition during ball milling, conventional sintering and spark plasma sintering for sub-micrometer or nano-metric (60h milling) of the composites were investigated in detail by X-ray diffraction (XRD), scanning electron microscopy (SEM) and EDS analysis. The maximum densification of $\text{ZrB}_2\text{-B}_4\text{C-Mo}$ ceramic matrix composite was achieved at 1800°C . The composites prepared by spark plasma sintering at 1800°C records extraordinary level of improvement of the hardness (27.34GPa) which is 3-4 times of higher hardness value than that of the composites sintered at conventional techniques. Similarly, the ball on disc wear resistant property of $\text{ZrB}_2\text{-B}_4\text{C-Mo}$ ceramic matrix composite exhibits higher in the samples prepared by spark plasma sintering at 1800°C .

Keywords: $\text{ZrB}_2\text{-B}_4\text{C-Mo}$ ceramic matrix composite, Ball milling, X-ray diffraction (XRD), Scanning electron microscopy (SEM), Mechanical properties

Contents

Certificate	i
Declaration.....	ii
Acknowledgement	iii
ABSTRACT.....	iv
List of figures.....	vii
List of tables.....	ix
Chapter 1	1
Introduction.....	1
1.1 Introduction	2
1.2 Objectives of the research work	4
Chapter 2	5
Literature Review	5
2.1 Composite materials	6
2.2 Type of composite materials	6
2.3 Mechanically alloying	6
2.4 Processing of CMCs.....	7
2.4.1 Cold Pressing and Sintering	7
2.4.2 Slurry Infiltration/Impregnation	8
2.4.3 Spark plasma sintering.....	9
1.3 Advantages of Spark plasma sintering	10
2.5 Summary of relevant literatures	11
Chapter 3	17
Experimental Procedure	17
3.1 Synthesis of $\text{ZrB}_2\text{-B}_4\text{C-Mo}$ ceramic composite	18
3.1.1 Powder Preparation.....	18
3.1.2 Compaction.....	19
3.1.3 Sintering.....	20
3.1.3.1 Conventional Sintering	20
3.1.3.2 Spark plasma sintering	21
3.2 Microstructural characterization	22

3.2.1 X-ray diffraction	22
3.2.2 Scanning electron microscopy	23
3.2.3 Optical Microscopy	23
3.3 Mechanical Testing	24
3.3.1 Vicker's Hardness measurement	24
3.3.2 Wear study	25
3.3.3 Density measurements of sintered pellets	26
Chapter 4	27
Results and Discussions	27
4.1 X-Ray Diffraction (XRD) analysis	28
4.1.1 XRD analysis of powders during milling	28
4.1.2. XRD analysis of sinterd products	29
4.2 Scanning Electron Microscopy	31
4.2.1 SEM analysis of milled products	31
4.2.2 SEM analysis of sintered products	32
4.3 Relative density/apparent porosity analysis	36
4.4 Vickers hardness Test.....	39
4.5 Wear behavior of the sintered pellets	41
Chapter 5	44
Conclusions.....	44
5. Conclusions	45
Reference.....	47

List of figures

Serial Number	Figure Number	Figure description	Page Number
1	2.1	Schematic flow diagram of Slurry Infiltration Process	9
2	2.2	Schematic diagram of spark plasma sintering	10
3	2.3	SEM images of microwave sintered ZrB_2 containing 4.0 wt.% B_4C at different temperature (a)1630°C (b)1720°C (c)1820°C (d)1920°C .	12
4	2.4	Morphology of ZrB_2 -SiC by rapid heating at (a)1500°C (b)1600°C and (c) 1700°C.	14
5	2.5	SEM images of SPS sintered samples at 1800°C (a) as-received ZrB_2 (b) $(\text{ZrB}_2)_{95.1}(\text{ZrC})_{3.7}(\text{ZrO}_2)_{1.7}$ (c) $(\text{ZrB}_2)_{96.8}(\text{ZrC})_{3.2}$ (d)low magnification microstructure of the $(\text{ZrB}_2)_{95.1}(\text{ZrC})_{3.7}(\text{ZrO}_2)_{1.7}$ composite	16
6	3.1	Ball milling	19
7	3.2	Single acting cylinder compaction machine	19
8	3.3	Tubular furnace is used for conventional sintering	20
9	3.4	schematic diagram of spark plasma sintering	21
10	3.5	XRD machine used for X-ray diffraction of the samples	22
11	3.6	Scanning Electron Microscope (SEM) model-JSM 6480LV,make-JEOL	23
12	3.7	Optical microscopy with Image analyzer	24
13	3.8	Vicker's Hardness Tester	25
14	3.9	Specimen showing indentation	25
15	3.10	Ball-on- disc wear testing machine	25
16	4.1	XRD spectra of milled powders of ZrB_2 - B_4C -Mo at different milling time: (a) 0h, (b) 42h and (c) 60h	28-29
17	4.2	XRD patterns of ZrB_2 - B_4C -Mo ceramic composite sinterd at different temperatures: (a)1500°C, (b) 1600°C and (c) 1800°C	30-31

18	4.3	SEM Image of the milled powder of $\text{ZrB}_2\text{-B}_4\text{C-Mo}$ at different milling times.	32
19	4.4	SEM Images of the sintered pellets of $\text{ZrB}_2\text{-B}_4\text{C-Mo}$ at 1500°C : (a) lower and (b) higher magnifications	33
20	4.5	SEM Images of the sintered pellets of $\text{ZrB}_2\text{-B}_4\text{C-Mo}$ at 1600°C : (a) lower and (b) higher magnifications	33
21	4.6	SEM images of $\text{ZrB}_2\text{-B}_4\text{C-Mo}$ composite sintered at 1800°C by plasma sintering for different magnification: (a) low and (b) high	34
22	4.7	Crossponding EDS spectrum of the bright phase showing the elemental peaks of Zr and B.	35
23	4.8	Crossponding EDS spectrum of the bright phase showing the elemental peaks of B and C.	35
24	4.9	SEM images of melted region of $\text{ZrB}_2\text{-B}_4\text{C-Mo}$ composite sintered at 1800°C by plasma sintering for different magnification: (a) low and (b) high showing dendritic structure.	36
25	4.10	Variation of density of $\text{ZrB}_2\text{-B}_4\text{C-Mo}$ composites with function of sintering temperatures.	38
26	4.11	The apparent porosity and bulk density of sintered $\text{ZrB}_2\text{-B}_4\text{C-Mo}$ composite.	38
27	4.12	Variation of hardness of sintered $\text{ZrB}_2\text{-B}_4\text{C-Mo}$ composites with the function of sintering temperatures	39
28	4.13	Variation of wear depth with sliding time for $\text{ZrB}_2\text{-B}_4\text{C-Mo}$ composites for different sintering temperature.	41
29	4.14	Optical microstructure of the worn surfaces of samples sintered at: (a) 1500°C , (b) 1600°C and (c) 1800°C , respectively.	42

List of tables

Serial Number	Table Number	Table description	Page Number
1	3.1	Ball Milling Parameter utilized	18
2	3.2	Spark plasma sintering parameter used	21
3	4.1	Summary of the EDS results of different phases in the microsturcures	35
4	4.2	Relation between sintering temperature and hardness of sintered pellets	41

Chapter 1

Introduction

1.1 Introduction

ZrB₂ is an ultra-high temperature ceramic with high melting point i.e. 3246°C, its hardness is more than the 500MPa. Over the last few years ZrB₂ceramic based composites are extensively used due to their best mechanical properties. It has superior electrical conductivity, corrosion resistance and also chemical stability against molten metal and non-basic slags [1-4].In view of these properties the main applications of ZrB₂ ceramic are in cutting tools, thermal protective systems, aero-crafts, crucibles which consist molten-metals and high temperature electrodes [5].

It is very difficult to make dense ZrB₂ materials at low temperature due to its high melting point and strong covalent-bonding. Densification of ZrB₂ involves usage of additives, without which the densification process will have to be carried out at high sintering temperatures of the order of 2100°C to 2300°C [6]. ZrB₂ ceramics have low fracture toughness 2.4 to 3.5 MPam^{1/2}and hence its applications are limited [7]. Therefore it is very important to develop a low-temperature process to produce ZrB₂ based ceramics with high toughness. To improve its fracture toughness researchers have added second phases like SiC_p [8], SiC_w[9], ZrSi₂[10] , ZrC[11], CNT[12] and B₄C[1]but it has been found that in most cases no improvement of fracture strength has been observed. Hence, improving both fracture toughness and strength of ZrB₂ based ceramics requires addition of some metal material. Also addition of metal material into these ceramics will result in improved densification even at low temperature [13, 14].

Among other ceramics such as diamond boron nitride, cubic boron nitride, B₄C (Boron carbide) occupies third position with respect to hardness and also abrasion resistance [15-17]. But at elevated temperatures (>1300°C) B₄C has low density (2.52 g/cm³) and high hardness (35 to

45GPa), so it is an ideal for applications requiring high temperature wear resistance. Other advantages of boron carbide include low cost, high neutron absorption ability, abundance of its raw material [18]. Zirconium di-boride (ZrB_2) and Boron carbide (B_4C) have interesting properties, and by mixture of these two ceramics there is chance of covering each other's limitations related to physical and mechanical properties. Due to this reason, researchers have taken interest in examining the ZrB_2 - B_4C composite. In recent years, work has been carried out such that any one of them was taken as matrix and another one taken as reinforcement. To consolidate ZrB_2 - B_4C composite powders sintering techniques namely hot pressing, pressure-less sintering and microwave sintering are being used in recent years. Since, adding metal powders (such as Cr, Mo, W and Ni) improve densification of ZrB_2 based ceramics incorporating a third phase into ZrB_2 - B_4C composite is necessary [13, 14]. Among these metals Molybdenum (Mo) was the choice of researchers because of its low density (10.2 g/cm^3), high melting point (2610°C)[19] and low thermal expansion coefficient ($6 \times 10^{-6} \text{ K}^{-1}$), which is very close to that of ZrB_2 ($6.88 \times 10^{-6} \text{ K}^{-1}$)[20,21]. These properties make Mo suitable for low-temperature preparation of ZrB_2 based materials with high density and high fracture toughness. To the best of our knowledge, the sintering performance and properties of the ZrB_2 - B_4C -Mo system have not been reported so far yet.

1.2 Objectives of the research work:

- (a) To synthesize $\text{ZrB}_2\text{-B}_4\text{C-Mo}$ ceramic matrix composite by mechanical alloying and sintering (conventional and SPS).
- (b) To study the effect of sintering temperature on the $\text{ZrB}_2\text{-B}_4\text{C-Mo}$ pellets.
- (c) Characterization of milled powders as well as sinter products by using XRD, SEM and EDS analyses.
- (d) To study of mechanical properties such as hardness and wear resistance of bulk $\text{ZrB}_2\text{-B}_4\text{C-Mo}$ ceramic matrix composites.

Chapter 2

Literature Review

2.1 Composite materials

The composite materials obtain from combining the two or more different materials to achieve desired properties that the each component cannot be attained by themselves.

2.2 Type of composite materials

1. Metal matrix composite (MMC)
2. Polymer matrix composite (PMC)
3. Ceramic matrix composite (CMC)

The aim of the developing Ceramic matrix composites (CMC) is to improve the ceramic desirable properties by incorporating reinforcements in them and limiting their inherent weaknesses. Development of CMCs imparts various improvements over ceramics such as:

- Capability of dynamic load is higher
- Degree of anisotropy on incorporation of fibers
- Improved fracture toughness
- Elongation to rupture up to 1%

2.3 Mechanically alloying:

Mechanical alloying (MA) is the solid-state powder processing technique which involves re-welding of powder particles, cold welding and fracturing in the high-energy ball milling. In mechanically alloying process a small amount of the blended powder mixture is put on the

container along the grinder media such as stainless steel ball, zirconia ball and whole mass is agitated at a high speed for a predetermined length of time. Lubricant (also called process control agent) can be added occasionally, especially milling material is ductile. The Process control agent minimized the formation of the large lumps of powder and effect of cold welding. Alloying happens between the basic powders and homogeneous alloy is got toward the end of processing [22].

2.4 Processing of CMCs

Ceramic matrix composite materials can be produced by conventional sintering techniques utilized for making polycrystalline ceramic and also can be manufactured by new techniques such as spark plasma sintering, which is specifically for CMCs Making.[23]

2.4.1 Cold Pressing and Sintering

After the cold pressing of fiber and matrix powder, the green compact pellets followed by sintering are carried forward by conventional sintering processing of ceramic. Mostly in the sintering stage, the composite incurs lot of cracks due to the shrinkage of matrix. This shrinkage problem connected with the sintering of any type of ceramic. Few other problems arise when high-aspect ratio reinforcements are added to ceramic matrix material or a glass and attempted to sinter. Network formation takes place upon addition of whiskers and fibers, this network may restrict the sintering process. The difference in thermal expansion coefficients of matrix and reinforcement, may lead to hydrostatic tensile stress while cooling the matrix. The driving force for process of sintering gets affected by this hydrostatic tensile stress resulting in lower densification rate of the matrix [23]

2.4.2 Slurry Infiltration/Impregnation

Slurry infiltration process is one of the processing techniques used to fabricate ceramic matrix composites. In this process, composite is synthesized by infiltrating the matrix, which is present in the form of a slurry or liquid, in the fibre preform. Impregnation takes place in a container with matrix (slurry phase). The slurry typically consists of matrix powder, liquid carrier and an organic binder is shown in Fig. 2.1. Factors like type of binder and amount, particle size distribution, powder content and carrier medium play vital role in producing a composite part which is good in quality. of these parameters which affect the composite part quality, the matrix powder is the most important one as the liquid carrier and the organic binder are removed during the process. To control porosity in the composite part and for thorough impregnation the particle size of the matrix powder should be maintained such that it is less than the fibre diameter. The extent of Infiltration of matrix phase into the fiber preform can be improved by using certain wetting agents in the slurry. Soon after the process of infiltration, the liquid carrier is made to evaporate. Next stage in the processing of the composite involves consolidation by laying up the resulting prepreg on a tool. Prior to the start of consolidation process the organic binder must be burnt out. [23].

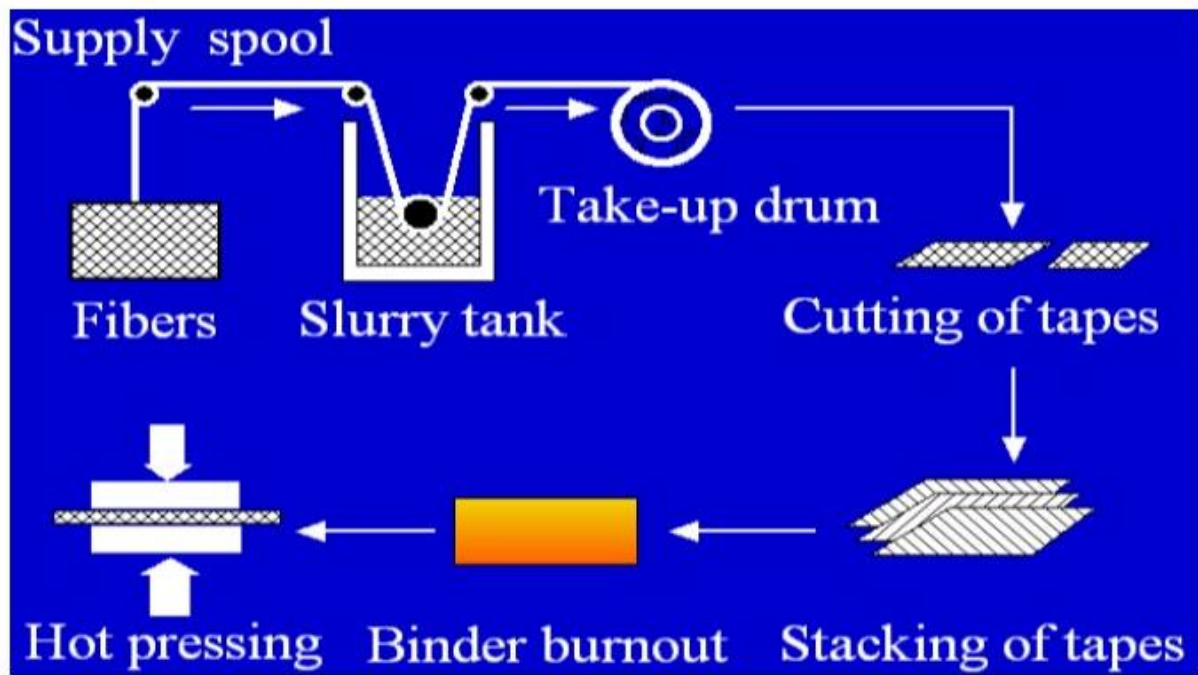


Fig. 2.1: Schematic flow diagram of Slurry Infiltration Process

2.4.3 Spark plasma sintering

Spark plasma sintering is a comparatively new technique that uses a pulsed direct current to heat the graphite pressure die and that allows very fast heating and cooling rates, short holding times and high pressures to obtain fully dense samples. In this newly developed technique of sintering the powders to be compacted are loaded in a die and a uniaxial pressure is applied while sintering (shown in Fig. 2.2). No use of external heating source is done in Spark plasma sintering. To heat the powder a pulsed direct current is allowed to pass through the electrically conducting die and the sample. In this process the die also acts as a heating source and the sample is heated from both inside and outside. Compaction of a wide variety of materials, e.g. functional graded materials, metals and alloys, composites and structural and functional ceramics are done by spark plasma sintering.

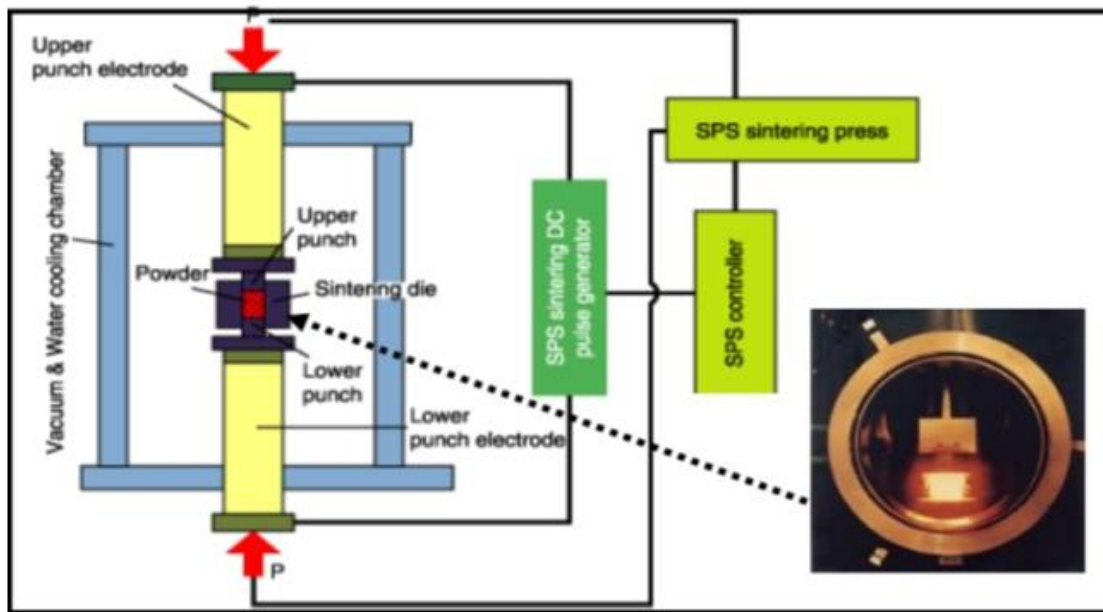


Fig. 2.2 Schematic diagram of spark plasma sintering

1.3 Advantages of Spark plasma sintering

(1) Spark plasma sintering (SPS) techniques are superior to the conventional sintering processes because it does not take so much time for the densification. In the conventional sintering processes external heating is performed over the sample, while in SPS internal heating is employed over the sample along with small holding time (5-10min) for the purpose of increase in sintering rate. In this sintering technique heating rates as high as $300^{\circ}\text{C}/\text{min}$ or more can be achieved in time period of 3-5 min. In the SPS techniques due to the high pressure along with high temperature higher rate of densification can be achieved, while in conventional sintering has no such rate of densification.

(2) No coarsening and grain growth are allowed to occur in this process, hence higher relative densities can be achieved, whereas in the case of conventional sintering does not allow so.

(3) Furthermore, in SPS the powder particle is generally poured into the die of graphite enclosed by temporary punches in the presence of vacuum, Argon etc. while in conventional sintering

processes, first a green compact is produced with the external dies and then it is introduced in furnace for sintering. In the former case it is easy to regulate the atmospheric conditions but in the later one it is not possible to do so.

(4) SPS does not permit to have any type of unwanted reactions during the sintering operations, so prevent the formation for unnecessary product which can be obtained in case of conventional sintering processes.

2.5 Summary of relevant literatures

Z. Sumin et. al [24] has carried out microwave sintering of two different ceramic materials, ZrB_2 and B_4C , in the proportion of 96% and 4% respectively. It has been observed that relative density of the sintered product is more than 98% even at temperature of about 1720°C . The grain size of the ZrB_2 matrix was increased from 2 to $15.9\mu\text{m}$ with increase in microwave sintering temperature from 1630°C to 1920°C . Recent report shows (Fig. 2.3) that microwave sintering is superior to conventional sintering. In microwave sintering densification is achieved at lower temperature without significant grain growth. Recent literature shows that the Vickers hardness and fracture toughness of microwave sintered specimen of $(\text{ZrB}_2)_{96}(\text{B}_4\text{C})_4$ is about 17.5GPa and $3.8\text{MPa m}^{1/2}$ respectively.

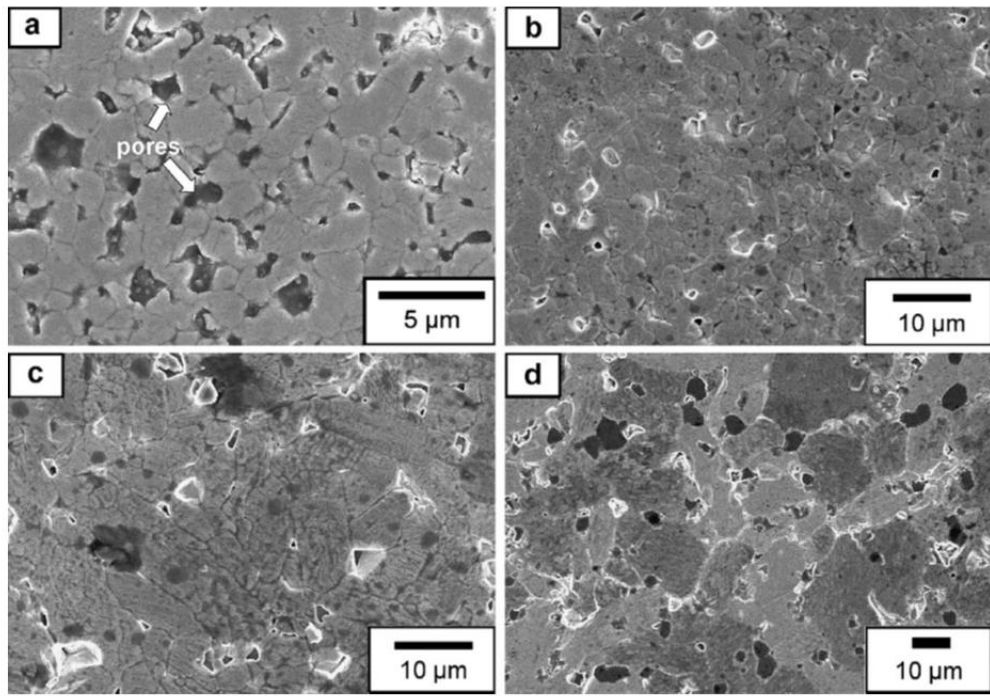


Fig. 2.3: SEM images of microwave sintered ZrB_2 (light grey phase) containing 4.0 wt.% B_4C (dark grey phase) at different temperature (a)1630°C (b)1720°C (c)1820°C (d)1920°C [24].

W Hailong et al [25] found that when ZrB_2 -Mo Ceramic composite are produced by hot-pressing sintering process at 1950°C with different volume fraction of Mo, there were two different samples, the first one with 5% volume fraction of Mo and 95% of ZrB_2 , another sample with 10% of Mo and 90 % of ZrB_2 volume fraction. Addition of Mo in ZrB_2 -Mo Ceramic composite is to improve densification and enhance mechanical properties of the composite. The high relative density of 98.9% is achieved in the case of ZrB_2 -Mo (10%vol) as compared to the pure ZrB_2 and ZrB_2 -Mo (5%vol) composite. As well as fracture toughness increased from 4.52 to 7.98 $\text{Mpa m}^{1/2}$ and bending strength from 424 to 450 Mpa in the case of ZrB_2 -Mo (10%vol) as compares to the pure ZrB_2 . Due to reduction in grain size and formation of MoB phase formation due to reaction of ZrB_2 and Mo, the mechanical properties of the ceramic composite have improved.

Huang S.G et al [26] Proposed that the B_4C - ZrB_2 (30wt. %) ceramic composite prepared by two different sintering processes, first set of sub-micrometer sized composite which was also mixed with black carbon powder was made by pulsed electric current sintering. Another set of B_4C - ZrB_2 powder alloy synthesized by conventional sintering at 1100 to 1400°C with 2hr holding time. The effect of the sintering temperature on chemical composition and evolution of phases in the composite were examined by SEM and X-ray diffraction analysis. In the case of conventional thermal process, fine grains, fully dense composite was achieved and a new ceramic phase ZrO_2 was formed. In the case of PECS process it was found that ZrB_2 in the initial stages of sintering reacted with B_4C and forms the B_2O_3 . Composites obtained by both the processes exhibit hardness in the range of 30 to 32 GPa. Moderate fracture toughness and high flexural strength, 2.4-2.9 MPa $m^{1/2}$ and 630-730 MPa respectively, of the composite produced by both the processes were achieved.

M Jalal Mousavi et al [27] has observed that with the help of Mo, C, and Fe as sintering additives, ZrB_2 ceramic powder was effectively densified by pressure less sintering process. Effect of these additives on densification, mechanical properties and microstructure of sintered pellets was examined. It was revealed that ZrB_2 - Mo (15wt. %)-Fe (10wt. %)-C (1wt. %) ceramic composite got maximum density. The fracture toughness and compressive strength of the ZrB_2 -Mo (10wt. %)-C (1 wt. %) were acquired as maximum 12.5 MPa $m^{1/2}$ and 425 MPa respectively. As well as fracture toughness has been improved at higher content of carbon i.e. 2wt. % in the case of ZrB_2 -Fe (10wt. %) composite.

Krishnarao R.V et al [28] suggested that in order to produce the ZrB_2 at different temperature in the range of 1020°C -1600°C (shown in Fig. 2.4), there should be a reaction between ZrO_2 with B_4C in absence of carbon. Also to generate single phase component ZrB_2 , the fraction ratio of ZrO_2 - B_4C should be optimized. If Silicon species are added to the composite ZrB_2 - SiC , ZrB_2 -

SiC–B₄C is formed in the powdered form. These silicon species when introduced by reaction it forms SiC and gets distributed uniformly in the whole mixture of ZrB₂ matrix. The powder can be coated by means of air plasma coating. The mixture of ZrO₂+B₄C+Si is suddenly heated in a continuous furnace at high elevated temperature, between the range of 900°C and 1700°C for 3–5 min. Generation of ZrB₂ along with SiC was found by means of XRD techniques and SEM analysis at a temperature equal to or above the 1300°C. In conclusion the agglomeration of powder particles takes place in the temperature range of 1300°C to 1700°C. Above 1700°C temperature, it is confirmed that tiny shaped particle exists (size in sub microns).

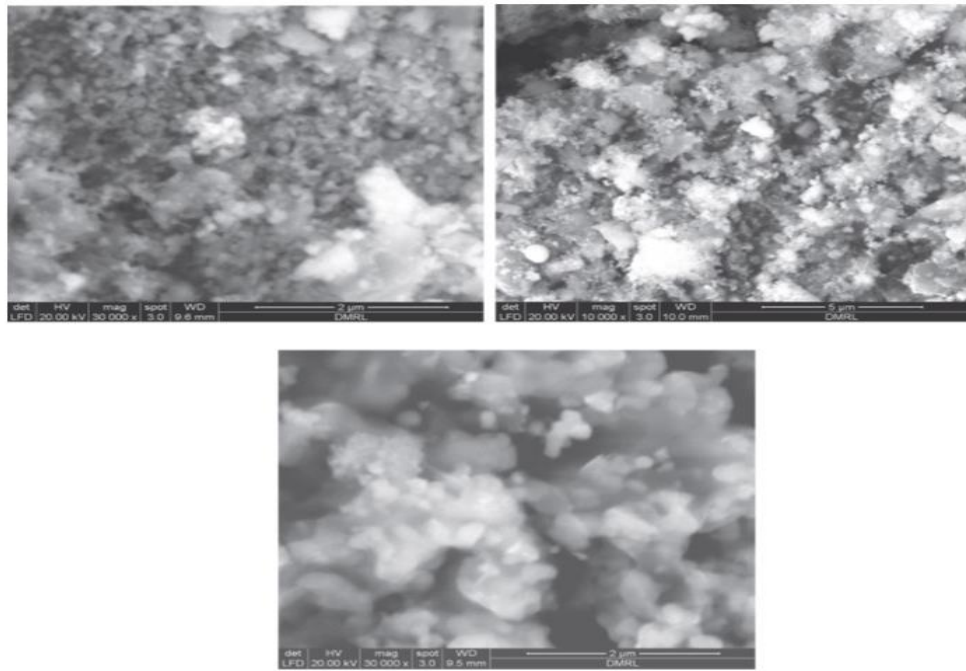


Fig. 2.4. Morphology of ZrB₂–SiC formed from (ZrO₂:B₄C:Si_{1/4}5:2:1) by rapid heating at (a) 1500°C (b) 1600°C and (c) 1700°C [28].

A Mehdi shahedi et al [29] focused on ZrB₂–B₄C composites for his research work on account of its stability at high temperature along with enormously high hardness. Due to high temperature involved during the sintering operation there were changes in the properties of ZrB₂–B₄C. The main focus of this research paper is regarding the porosity and densification of ZrB₂–B₄C

ceramic composites having 0 vol. % to 100vol. % B_4C (hot pressing is done at $1800^{\circ}C$ for a period of 30 min under a load of 12MPa). In order to get information about the fracture surfaces of specimen in addition with volume fraction of constituents during the sintering operation SEM analysis was carried out. Finally it is concluded that as the amount of B_4C increases there will be decrease in the density of the compact. Also porosity changes accordingly from closed to open structures. Furthermore, sintering processes can be regulated by means of ZrO_2 transient phase generated by means of heating operations.

Caen et al. [30] explains a method to produce high temperature composites with the help of powder metallurgy techniques integrated with a sol gel process (shown in Fig. 2.5). In this paper ZrB_2 powder is treated with coating of ZrO_2 -C- sol gel. After the carbothermal reduction ZrB_2 powder surface is covered by ZrC grains. In order to regulate the oxide reduction over the surface of ZrB_2 the carbon present in sol gel phase is refined. TEM, SEM & XRD techniques are the basic techniques by which microstructures as well as crystalline phases are analyzed. It has been observed that during the carbothermal reduction Nano- ZrC phase spreads over the surface of ZrB_2 completely at $1450^{\circ}C$. By means of sol-gel coating, homogeneous mixture of ZrC (200nm) over the surface of ZrB_2 is formed. In general spark plasma sintering is introduced in order to densify ZrB_2 - ZrC composite at the temperature of about $1800^{\circ}C$. The porosity as well as grain size can be regulated by means of regulating the carbon content in sol-gel precursor.

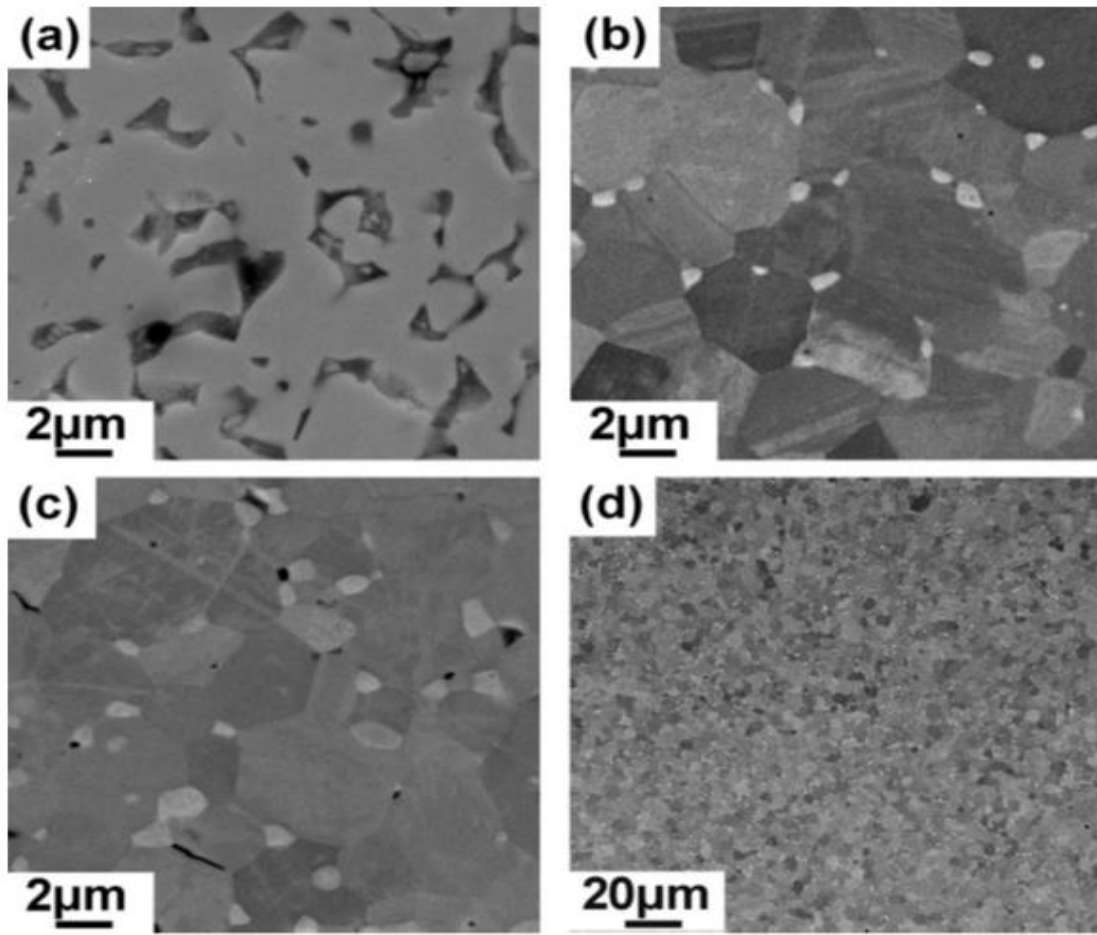


Fig.2.5: SEM images of SPS sintered samples at 1800°C (a) as-received ZrB_2 (b) $(\text{ZrB}_2)_{95.1}(\text{ZrC})_{3.7}(\text{ZrO}_2)_{1.7}$ (c) $(\text{ZrB}_2)_{96.8}(\text{ZrC})_{3.2}$ (d) a low magnification microstructure of the $(\text{ZrB}_2)_{95.1}(\text{ZrC})_{3.7}(\text{ZrO}_2)_{1.7}$ composite [30].

Chapter 3

Experimental Procedure

3.1 Synthesis of ZrB₂-B₄C-Mo ceramic composite

3.1.1 Powder Preparation:

The raw powders like ZrB₂ (ESK Ceramics GmbH & Co.Kg, Germany], boron carbide (Ceratech Trading Limited, Sanghai, China) and Molybdenum (Koch-Light Laboratories ltd. UK) have a particle size 35 μ m,20 μ m,4 μ m respectively Powders were the beginning material for synthesis by mechanical alloying. The alloy powder containing ZrB₂ (40 vol. %), B₄C (40 vol. %) and Mo (20 vol. %) are ball milled by utilizing zirconia ball media and toluene as grinding aid/coolant, at speed 350 rpm for 0 -60 hours (shown in Fig. 3.1). The green binder used in this process was PVA (Polyvinyl alcohol). There were three sets of powder synthesis, one alloy powder in micrometer size (avg. particle size \approx 32 μ m) taken before mechanical milling, second alloy powder in sub-micrometer size-1(average particle size \approx 20 μ m) produced by 42 hours of milling and third alloy powder in sub-micrometer sized-2 (\approx 12 μ m) produced by 60 hours of milling. The milling parameters are summarized in Table 3.1.

Table3.1: Ball Milling Parameters utilized

Mill type	High energy dual drive planetary ball mill
Grinding aid	Toluene
Milling speed	350rpm
Grinding media	Zirconia ball
Milling time	0h,42h,60h
Ball to powder ratio	4:1
Jar volume	100ml
Ball diameter	3mm



Fig.3.1: Ball milling

3.1.2 Compaction:

Dry milled powders (all un-milled, 42h and 60h of milling) were mixed with binder named polyvinyl alcohol (PVA) to help strong compaction and to get bonding tendency. Each sample consists of 12g of milled powder mixed with the 4 ml of polyvinyl alcohol (PVA). The green compaction was done of binder mixed milled powders was carried out by using the single acting cylinder compaction machine (Fig. 3.2) with diameter of 9.5 mm at an applied pressure of 6 ton. The dwell time for each pressing was 120 s.



Fig.3.2: Single acting cylinder compaction machine.

3.1.3 Sintering

3.1.3.1 Conventional Sintering

The sintering of green compacts of sub-micrometer sized (60h of milling) size powders were carried out in a tubular furnace (Okay, Model no. 7017) (shown in Fig. 3.3) under the argon atmosphere. First tube was evacuated to a vacuum level of 10^{-5} bar and the specimens were placed on a crucible inside the chamber. All samples were sintered at 1500°C with holding time for 3 hours in Ar atmosphere.

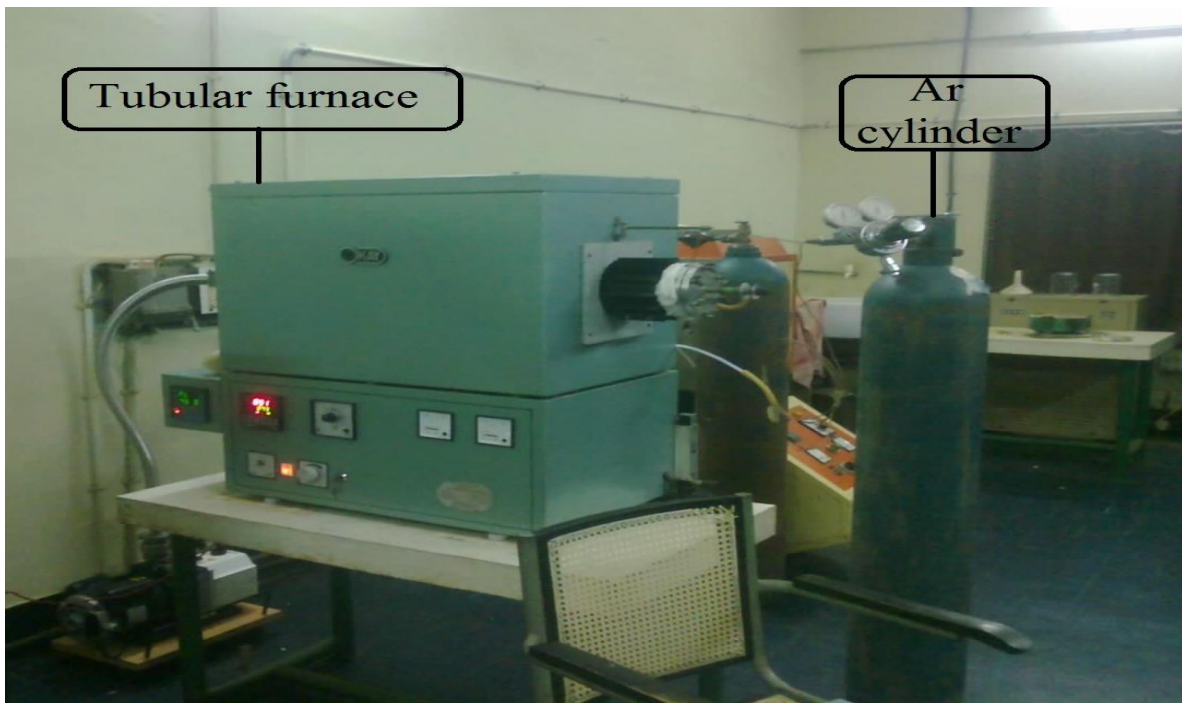


Fig.3.3: Tubular furnace is used for conventional sintering

3.1.3.2 Spark plasma sintering

Dry pellets of milled powder (60h) are placed on the bottom holding graphite plate by centering the pellet with respect to graphite rod attached to the system (shown in Fig. 3.4). The graphite rod is made in such way that it is hollow cylindrical in shape and the tip of the rod is connected by means of a small nozzle to provide atomizing behavior of argon gas during sintering process.



Fig. 3.4: spark plasma sintering equipment.

Following parameters are taken care during whole process and summarized in Table 3.2.

Table 3.2: Spark plasma sintering parameters.

DC Voltage	20-40 Volt
Current	100-160Ampere
Argon rate	2.5litre/min
Sintering time	30sec-1min

To avoid oxidation behavior Argon will pass through continuously in the nozzle for 5 min after sintering. After constant flow of argon gas, reducing atmosphere was created around the pellet area to make proper sintering and avoiding oxidation behavior of the sample. Then according to above mention parameters sintering process carried out.

3.2 Microstructural characterization

3.2.1 X-ray diffraction

The different of milling time of powder sample (0h(un-milled), 42h,60h) and polished sintered composite at various sintering temperature were characterized through modal ULTIMA-IV XRD system (shown in Fig. 3.5) by utilizing Cu-K α ($\lambda=1.5418^\circ$) radiation to focus the phase evolution at various level of milling material and various sintering conditions. 20° - 100° and 10° - 60° range of scanning has been taken for scanning. And step size $5^\circ/\text{min}$ has been taken.



Fig 3.5: XRD machine used for X-ray diffraction of the samples.

3.2.2 Scanning electron microscopy:

The microstructure of milled powder and sintered pellet observed by using of scanning electron microscopy (SEM,model-JSM 6480LV, make-JEOL) (shown in Fig. 3.6).Utilizing standard metallographic strategies all sample polished by mechanically before examination. Before examine sample coating has been done.



Fig 3.6: Scanning Electron Microscope (SEM) model-JSM 6480LV,make-JEOL

3.2.3 Optical Microscopy:

Fracture surfaces after ball on disc wear testing for sintered pellet at different temperature are observed by using optical microscope make-ZEISS, model- AxioCam ERc 5s (shown in Fig. 3.7).. In this optical the microstructures of ball on disc wear sample were analyzed with different magnification.



Fig 3.7: Optical microscopy with Image analyzer

3.3 Mechanical Testing

3.3.1 Vicker's Hardness measurement

Vickers's hardness tester is used on account of measurement of hardness. It has an indenter of square based pyramid of vertex angle 136° . It is also called the diamond-pyramid hardness test due to the shape of the indenter is diamond. Vickers hardness number is calculated by load divided by surface area of the indentation. VPH (Vickers's-pyramid hardness) number is calculated (Eq. 3.1) by using following equation:

$$\mathbf{VPH} = \frac{2P \sin(\theta/2)}{L^2} \quad (3.1)$$

Where L is the avg. length of diagonal in mm, P= applied load in Kg and θ =angle in between opposite face of diamond as 136° . Hardness of sintered specimens was carried out using Vickers' Hardness Tester (Fig. 3.8), dwell time of 10 sec. and load of 1 kg. The crack is found at the corner of the indentation shown in Fig. 3.9.



Fig 3.8: Vicker's Hardness Tester

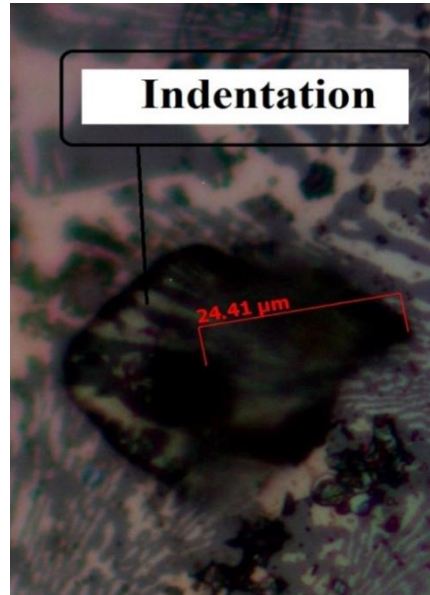


Fig.3.9: Specimen showing indentation

3.3.2 Wear study

Ball-on-plate wear tester (Ducom, TR-208 M1) machine (shown in Fig. 3.10) was used to performing the wear behavior of all the sintered pellets at different sintering temperature. The stainless steel ball in the dimension of 4 mm diameter rotates on the sintered pellet as shown in Fig 3.10 with the speed of 20rpm for 10 minutes under 20N constant load.



Fig 3.10: Ball-on- disc wear testing machine

3.3.3 Density measurements of sintered pellets

The theoretical density of the sintered samples was determined by using the rule of mixtures. The experimental density or bulk density of the sintered pellets was determined by Archimedes' method. Apparent porosity is the percentage of the total volume of a material occupied by both open and closed pores. To measure bulk density and apparent porosity of the mentioned composites, the dry weight of specimen was first measured. Then they were soaked in distilled water inside a beaker and after 90 minutes the specimens were taken out and soaked weight were calculated. After that the suspended weight was measured in kerosene.

The following equation using for determine relative density, experimental density and apparent density.

$$\text{Relative density} = \frac{\text{Experimental density}}{\text{theoretical density}} \times 100 \quad (3.2)$$

$$\text{Experimental density} = \frac{\text{Dry weight}}{\text{Soaked weight} - \text{dipped weight}} \quad (3.3)$$

$$\text{Apparent density} = \frac{\text{Soaked weight} - \text{dry weight}}{\text{soaked weight} - \text{dipped weight}} \times 100 \quad (3.4)$$

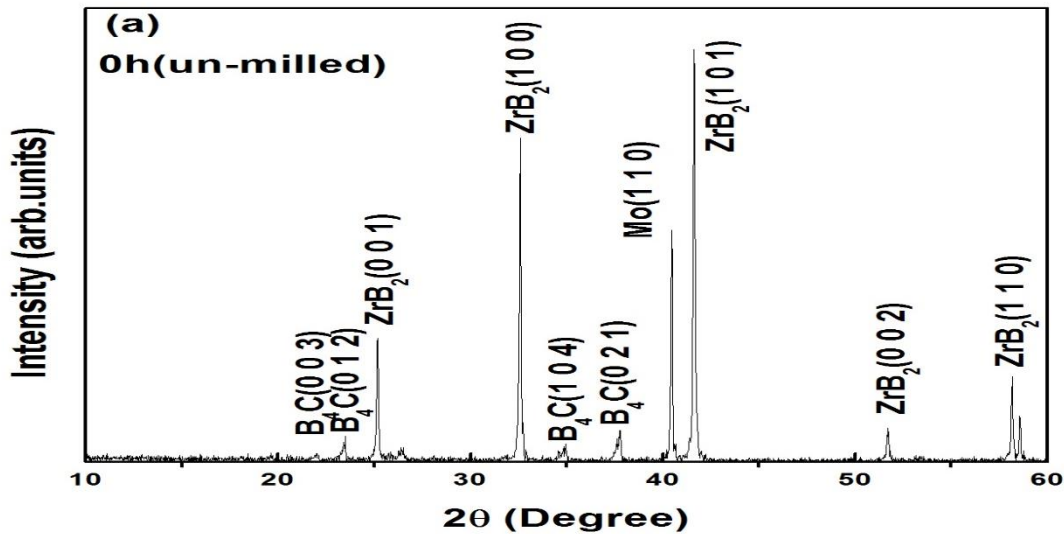
Chapter 4

Results and Discussions

4.1 X-Ray Diffraction (XRD) analysis:

4.1.1 XRD analysis of powders during milling

Fig.4.1a to c show that the X-ray diffraction spectrum of $\text{ZrB}_2\text{-B}_4\text{C-Mo}$ milled powders taken at different time like 0h (un-milled), 40h and 60 h, respectively. It reveals that from the analysis of XRD pattern that intensity gradually decreases with increase of milling time. Also found with slightly increase in peak width with increase in milling time. The increment in peak width is because of introduce the lattice strain and decrease in particle size (avg. particle size reduce $32\mu\text{m}$ to $12\mu\text{m}$). It is clear from the XRD patterns that the presence of ZrB_2 , B_4C and Mo phases of each stage milling. For XRD analysis of milled powders at higher milling time (40h and 60 h) shows the peak shifting as well as peak gets broadening, this due to the fact micron-level powder gradually reduce their size into sub-micron or Nano-metric level due fragmentation of particles caused by high energy ball mill.



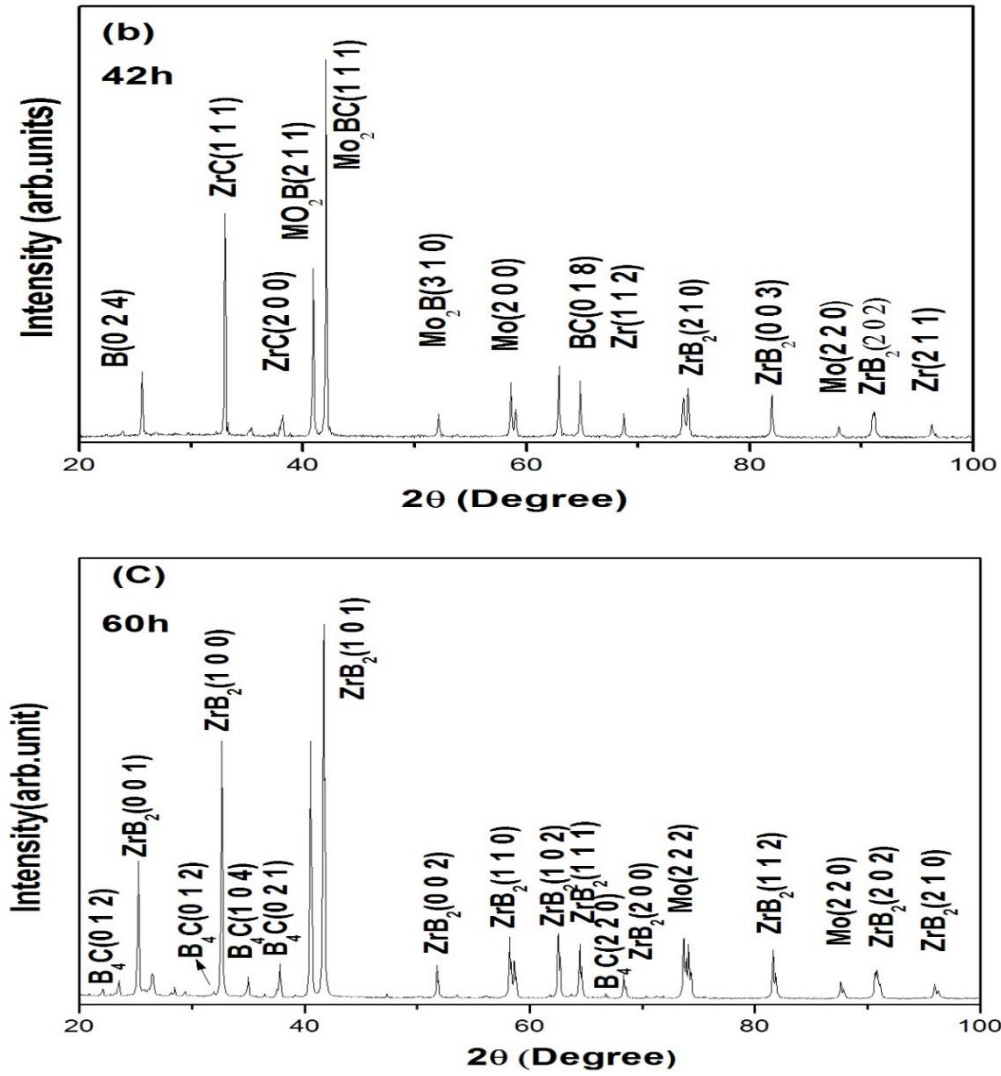
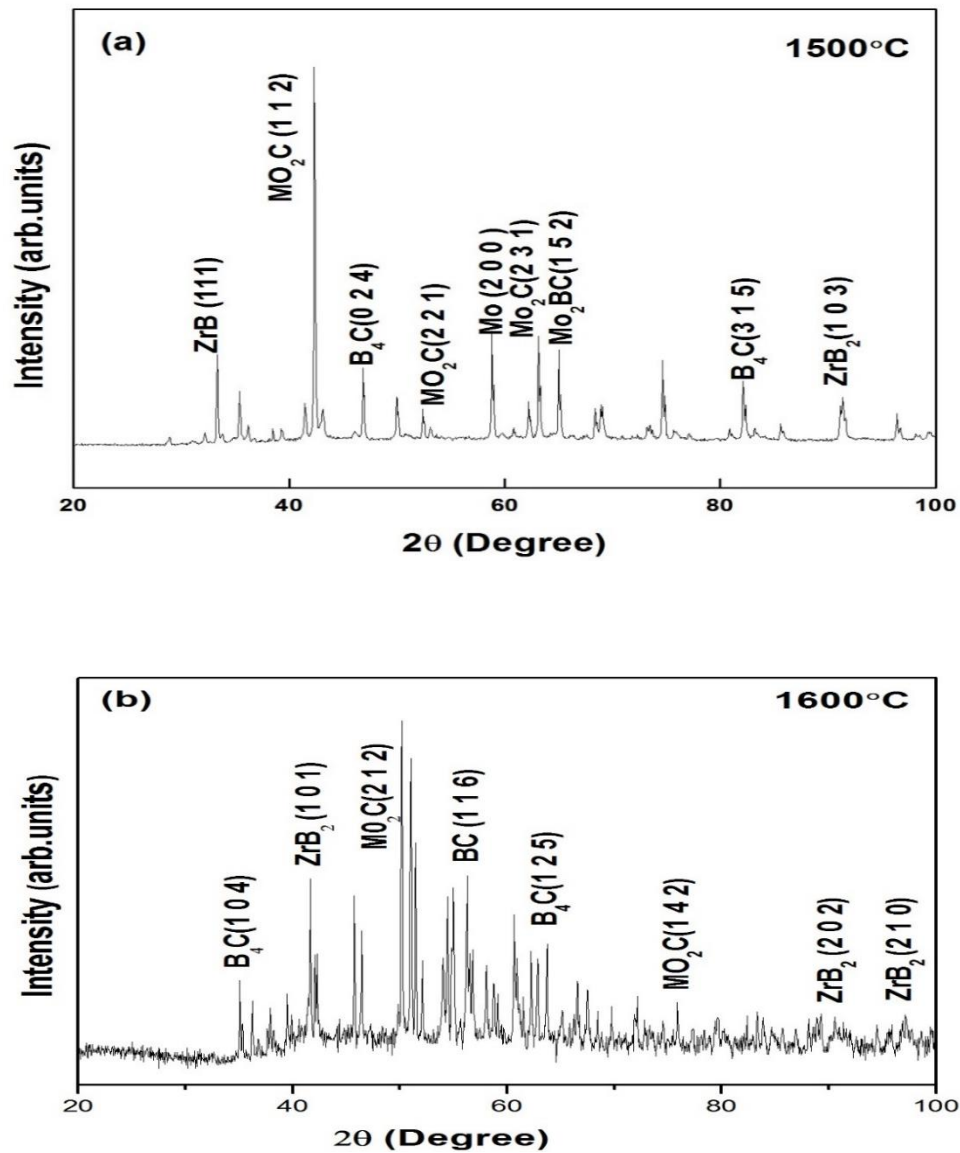


Fig. 4.1: XRD spectra of milled powders of $\text{ZrB}_2\text{-B}_4\text{C-Mo}$ at different milling time: (a) 0h, (b) 42h and (c) 60h.

4.1.2. XRD analysis of sinterd products

Fig. 4.2a and b show the XRD patterns of $\text{ZrB}_2\text{-B}_4\text{C-Mo}$ composite sintered at 1500°C and 1600°C in a tube furnace in the presence of argon atmosphere for 3.0 hrs. It is evident that the presence of predominant phases like ZrB_2 and B_4C along with some intermetallic phases like MoB and $\text{Mo}_2\text{CMo}_2\text{BC}$ in the sinterd product. On the other hand, the XRD analysis of $\text{ZrB}_2\text{-B}_4\text{C-Mo}$ composite sinterd at 1800°C at plasma sintering technique for holding time of 30sec-1min

(Fig.4.2c) shows similar kind of phases along with intermediate phases like zrc,MoB, Mo₂B. but the XRD peaks show the boarden in nature. The reason behind this advenced sintering is that at very small holding time the grain growth is not possible.



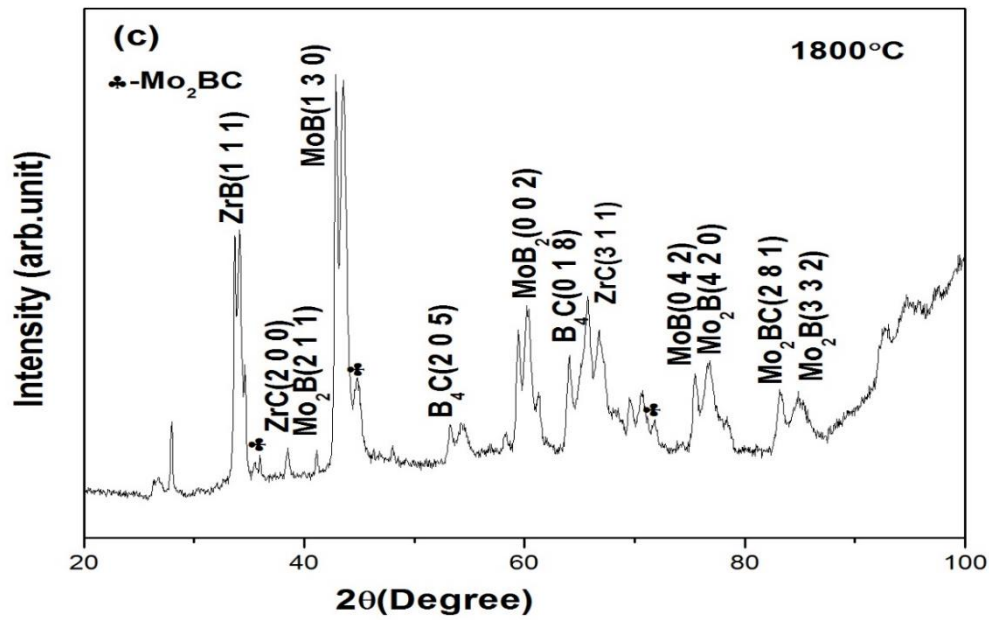


Fig 4.2: XRD patterns of ZrB₂-B₄C-Mo ceramic composite sinterd at different temperatures: (a)1500°C, (b) 1600°C and (c) 1800°C'

4.2 Scanning Electron Microscopy:

4.2.1 SEM analysis of milled products

Fig.4.3 reveals that the SEM microstructure of ZrB₂-B₄C-Mo milled powders at different stages of milling (0 h (un-milled), 42 h and 60h). It is clearly evident from the figure that the micron size powder get reduces into sub-micron or nano-meter level with increase in milling time. It has been observed that initial size of particle is of (<32μm), due to the milling, particle size is reduced and become of size around 5-10μm.

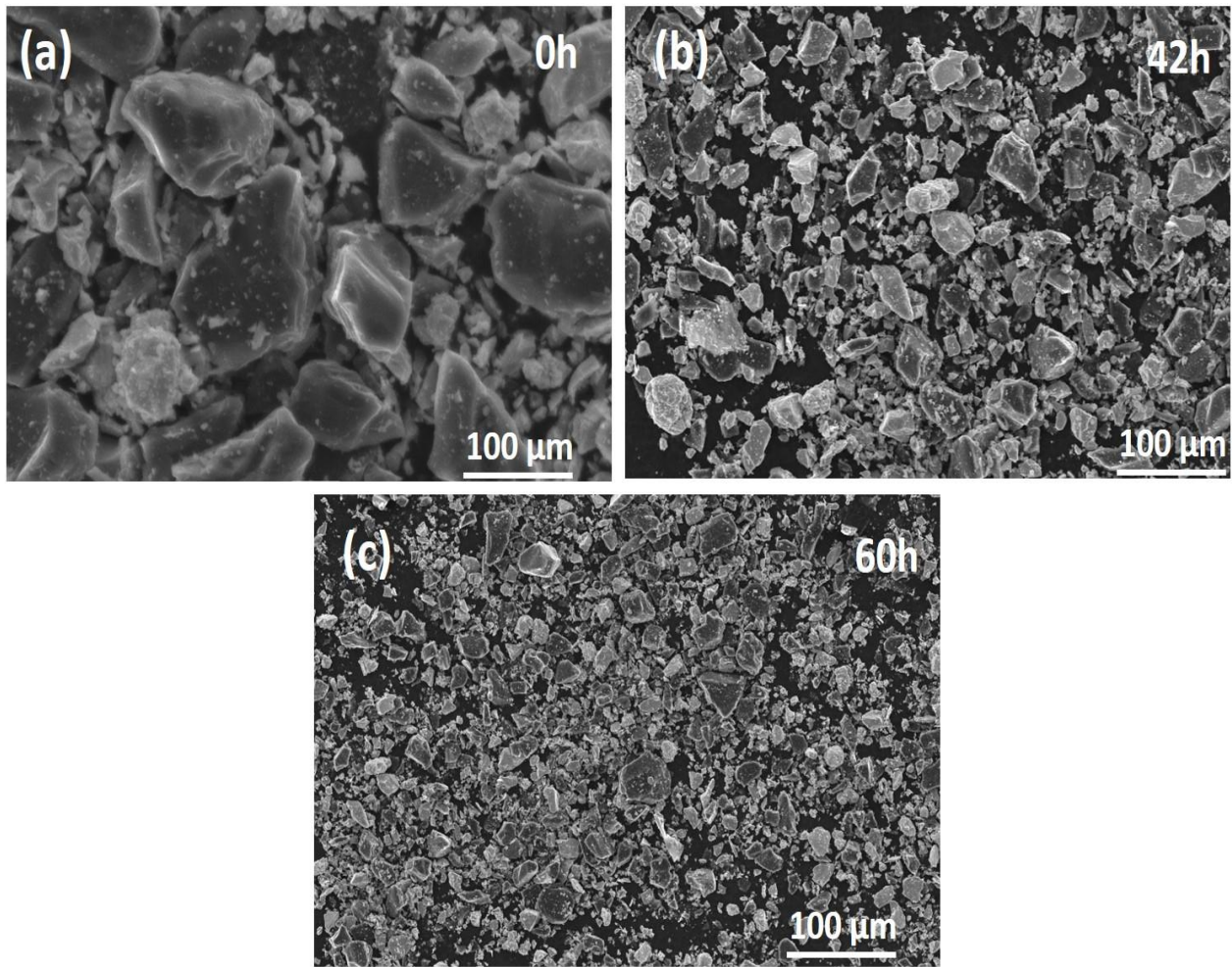


Fig 4.3: SEM Image of the milled powder of $\text{ZrB}_2\text{-B}_4\text{C-Mo}$ at different milling times.

4.2.2 SEM analysis of sintered products

Fig 4.4 shows that the SEM image of $\text{ZrB}_2\text{-B}_4\text{C-Mo}$ composite sintered at 1500°C in a tubular furnace in argon atmosphere for 3 hrs. It reveals that the partial sintering happens which confirms that the particles are not bonded properly. Similar kind of trends was found in the samples sintered at 1600°C in conventional technique for 3 hrs which are shown in Fig 4.5. It is clear that in the second case, the percentage of sinterability is higher than that of samples sintered at 1500°C . As a result of that, there is presence of porosity in the microstructures in

both cases. The partially sintered matrix this is due to that there the sintering temperature is not sufficient to make a strong bonding with the particles.

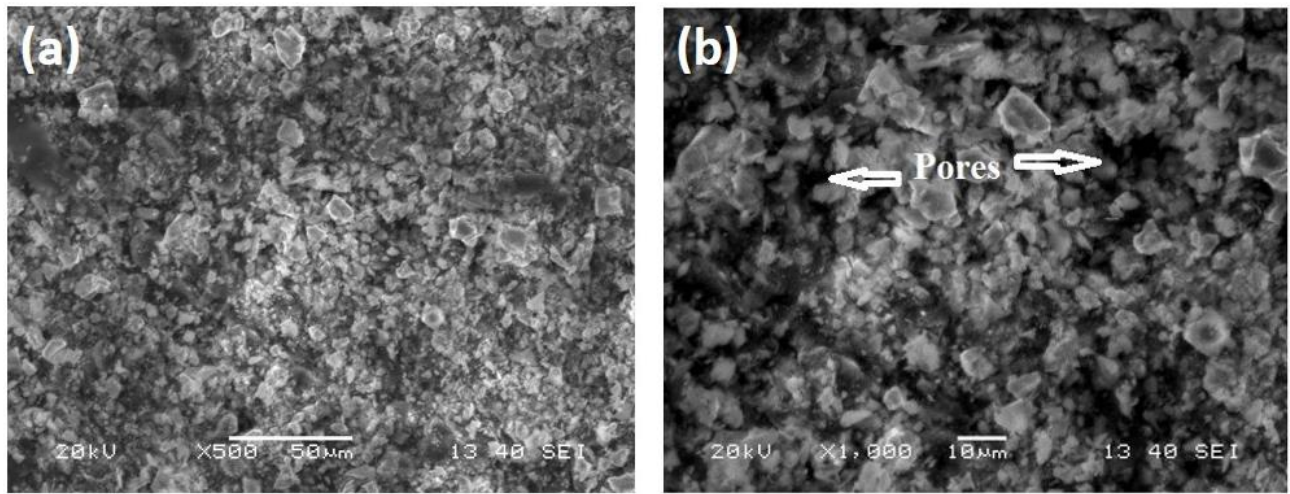


Fig 4.4: SEM Images of the sintered pellets of $\text{ZrB}_2\text{-B}_4\text{C-Mo}$ at 1500°C : (a) lower and (b) higher magnifications.

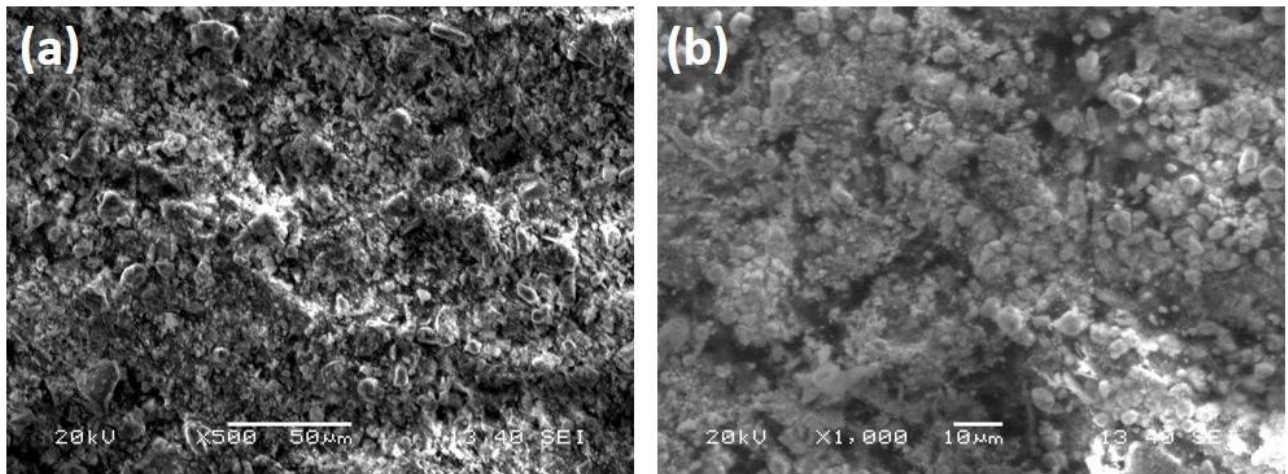


Fig 4.5: SEM Images of the sintered pellets of $\text{ZrB}_2\text{-B}_4\text{C-Mo}$ at 1600°C : (a) lower and (b) higher magnifications.

The best results have been revealed during the sintering of $\text{ZrB}_2\text{-B}_4\text{C-Mo}$ milled powder was done in plasma sintering technique. Fig 4.6 shows the microstructures of $\text{ZrB}_2\text{-B}_4\text{C-Mo}$ composite sintered at 1800°C in plasma sintering techniques for 30 sec-1min.. The figures reveal that the presence of bright phases i.e. ZrB_2 and dark phases i.e. B_4C in the microstructures of $\text{ZrB}_2\text{-B}_4\text{C-Mo}$ sintered at 1800°C .

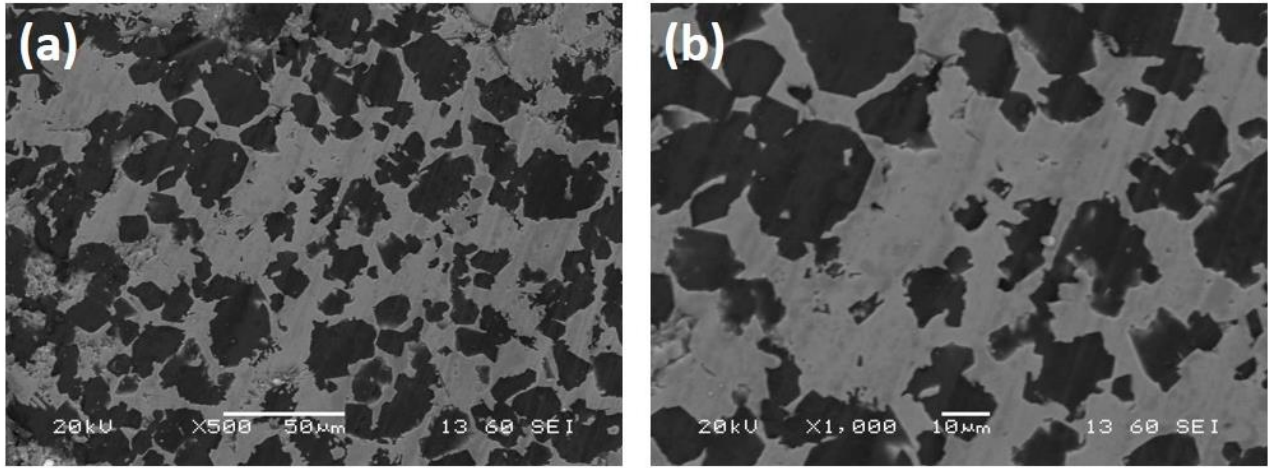


Fig 4.6: SEM images of $\text{ZrB}_2\text{-B}_4\text{C-Mo}$ composite sintered at 1800°C by plasma sintering for different magnification:(a) low and(b) high

Fig. 4.7 shows the corresponding EDS spectrum of the bright phase where predominant element Zr and minor element B present. On the other hand, for dark phase analysis (Fig. 4.8) shows the presence of C and B element. The elements present in the different phases are summarized in Table 4.1.

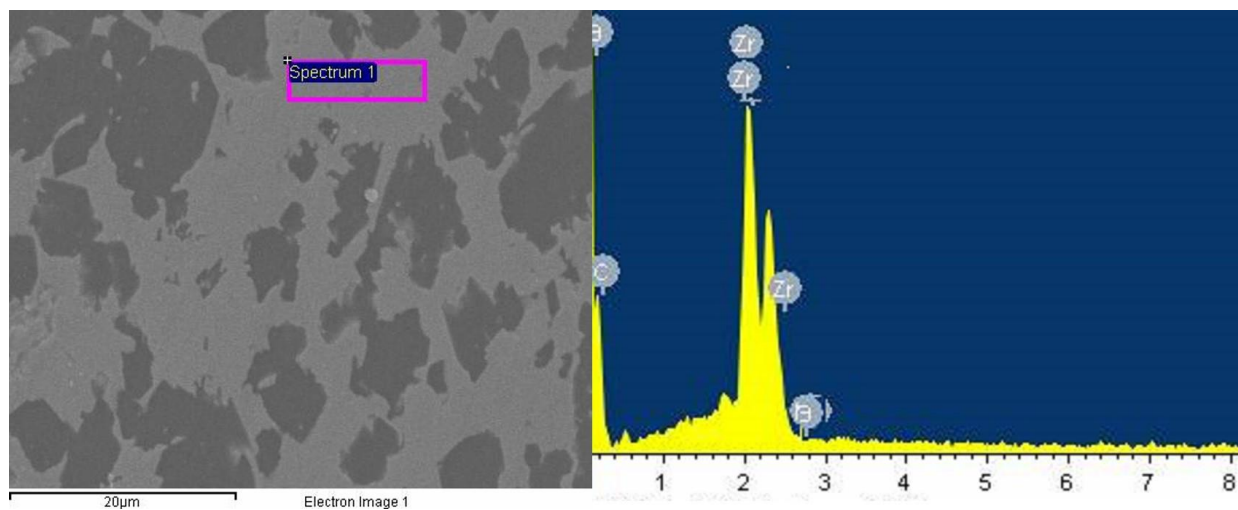


Fig. 4.7: Crosponding EDS spetrum of the bright phase showing the elemental peaks of Zr and B.

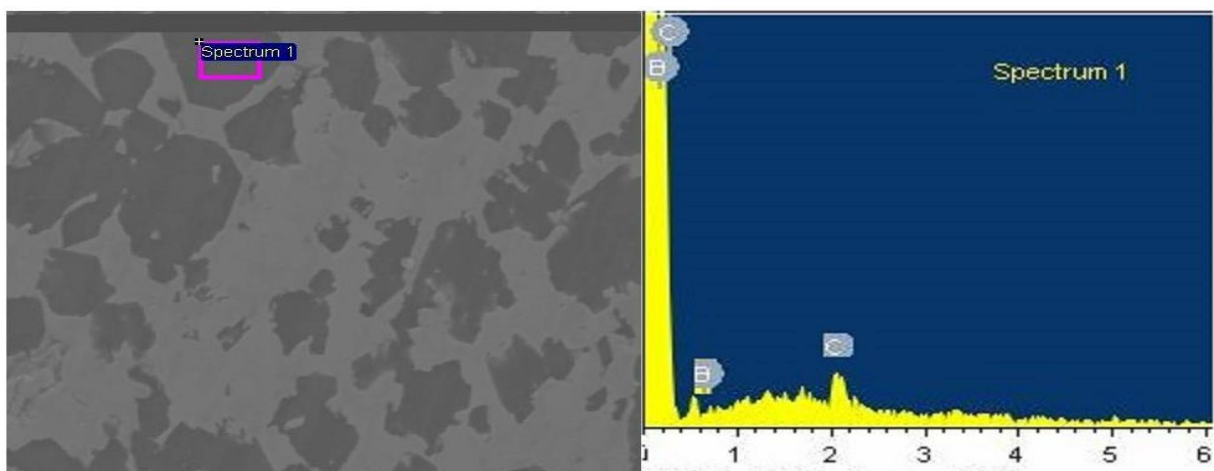


Fig. 4.8 Crosponding EDS spetrum of the bright phase showing the elemental peaks of B and C.

Table 4.1: Summary of the EDS results of different phases in the microsturcures

Element (Wt.%)	Bright Phase	Dark Phase
B	12.92	77.72
C	-----	22.28
Zr	87.08	-----

Fig 4.9 shows the microstructures of $\text{ZrB}_2\text{-B}_4\text{C-Mo}$ composite sintered at 1800°C in plasma sintering techniques for 30 sec results some the area of pellete melted due to high localized heat generated by plasma. It reveals the dendritic microstures where dark phase B_4C presence of interdendritic region of ZrB_2 . As a result of that the percentage of sinterability increases rapidly and produce very high dense products as compare that of sample sintered at 1500°C or 1600°C in conventional method.

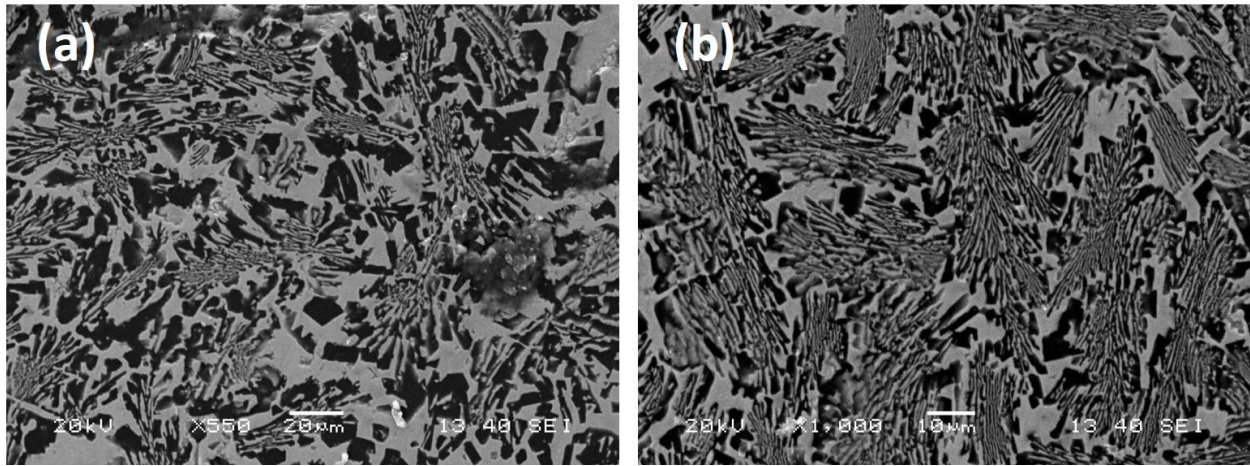


Fig 4.9: SEM images of melted region of $\text{ZrB}_2\text{-B}_4\text{C-Mo}$ composite sintered at 1800°C by plasma sintering for different magnification: (a) low and (b) high showing dendritic structure.

4.3 Relative density/apparent porosity analysis:

Fig. 4.10 shows the density variation with sintering temperatures of $\text{ZrB}_2\text{-B}_4\text{C-Mo}$ composites. It reveals that the samples sintered at 1500°C or 1600°C by conventional sintering method show lower density than that of samples sintered at 1800°C by plasma sintering method. It was observed that the samples sintered by conventional sintering showed incomplete sintering which results increase the amount porosity in the sintered products. But, samples sintered by

plasma sintering with higher temperature has showed complete sintered and also some portion has been melted due to localized increase in temperature which results in increase in density of the sintered products. The details of microstructure analysis is in reasonable good agreement with the discussion in section 4.2.2.

It has been found that the bulk densities increase with fineness of the ZrB_2 - B_4C -Mo composite mixture. Highest relative density achieved due to presence of ZrB_2 in the composite. The open-type porosity arises with increase in B_4C content, but the amount of closed-type porosity shows a reverse behavior. Densification behavior of ZrB_2 - B_4C -Mo composites has been improved remarkably by increasing sintering temperature by Spark plasma sintering technique, where temperature is in excess of 1800°C . With the progress of sintering process the nature of porosity changes gradually from open to closed form.

Therefore presence of negligible amount of open pores in ZrB_2 - B_4C -Mo cermet verifies that spark plasma sintering is much fruitful than conventional sintering. By using finer starting powder particles by subsequent ball milling, intensified the elimination of voids, Solid state diffusion becomes more pronounced during sintering and finally leads to sealing off the open channels between particles by efficient mass transport between powder particles. As a result the relative density of the composite material milled 60 hrs will give rise to nearby theoretical density while sintering through spark plasma technique.

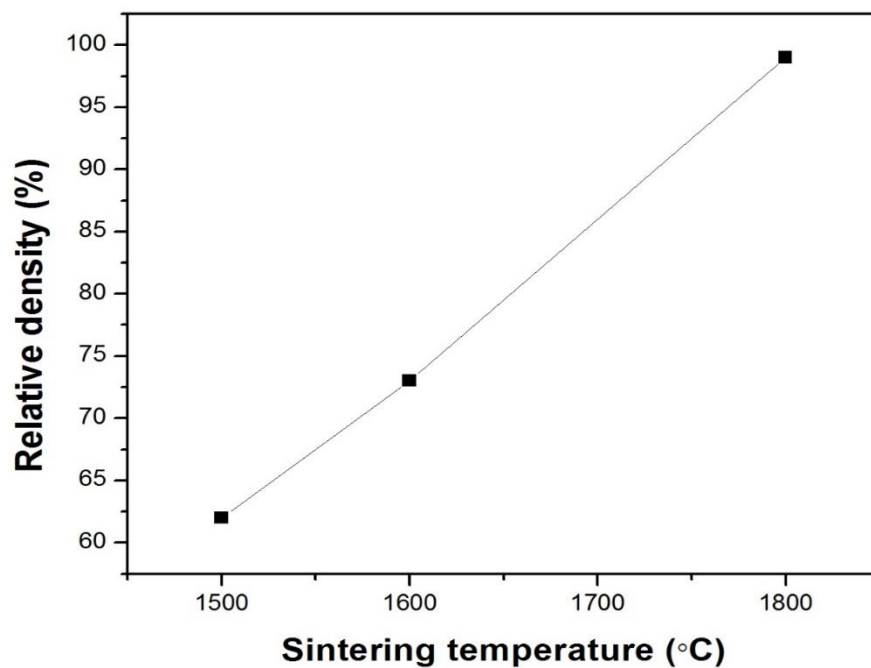


Fig. 4.10: Variation of density of ZrB₂-B₄C-Mo composites with function of sintering temperatures.

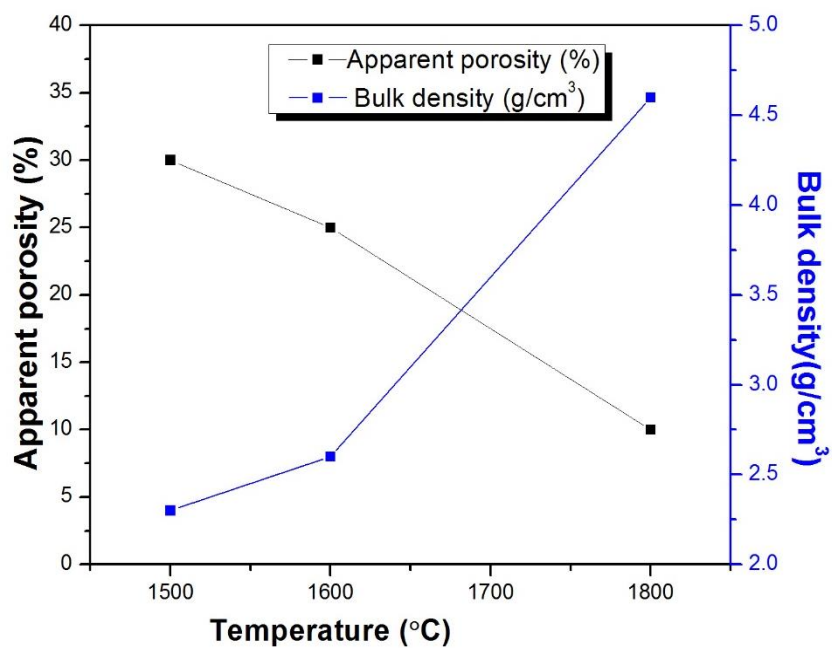


Fig. 4.11: The apparent porosity and bulk density of sintered ZrB₂-B₄C-Mo composite.

4.4 Vickers hardness Test:

Fig. 4.12 shows the variation of hardness of the $\text{ZrB}_2\text{-B}_4\text{C-Mo}$ ceramic composites as the function of sintering temperatures. It is evident from the figure that the hardness value is linearly increases with increasing the sintering temperatures. The previous section we have discussed that the density of the sintered pellets increase with the increasing in sintering temperature and maximum density have been achieved of sample sintered at 1800°C in plasma sintering process. By the same logic the hardness value of sample sintered at 1800°C in plasma sintering process recorded maximum as compared to that of samples sintered at 1500 or 1600°C .

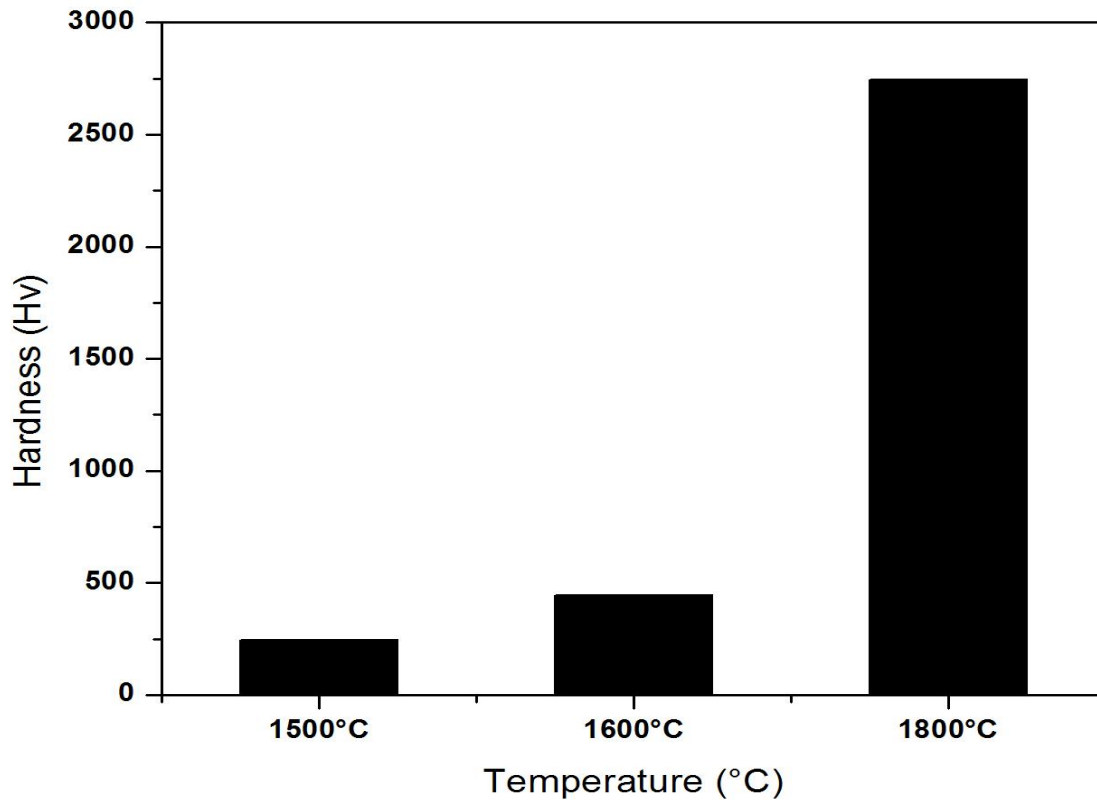


Fig. 4.12: Variation of hardness of sintered $\text{ZrB}_2\text{-B}_4\text{C-Mo}$ composites with the function of sintering temperatures

The hardness results of all the sintered samples are summarized in Table 4.2. From table it is clear that hardness value increments with expanding sintering temperature because of faster

diffusion at high temperature. As sintering temperature and milling time increases, bonding between particles improves and finally density and hardness increases.

From the graph (Fig. 4.12), the hardness of the composite increases from 234hv (2.3Gpa) to 2788hv (27.34Gpa) drastically, which was attributed to the decrease of porosity as the sintering temperature increased from 1600°C to 1800°C. Residual stresses in the sintered composite are another factor that may have contributed to the reduction in hardness. Since ZrB₂ has a hexagonal crystal structure with anisotropic thermal expansion coefficients ($6.88 \times 10^{-6} \text{ }^{\circ}\text{C}^{-1}$) [29], grain growth of specimen could have produced micro-cracking during cooling as a result of residual stresses. Hence, micro-cracking due to the anisotropic thermal expansion behavior of ZrB₂ may have accounted for the lower hardness. In addition, B₄C has an average thermal expansion coefficient of ($5.25 \times 10^{-6} \text{ }^{\circ}\text{C}^{-1}$) [29], which is lower than that of the ZrB₂-B₄C-Mo matrix. The thermal expansion coefficient mismatch between these individual elements could produce residual stresses near the ZrB₂-B₄C grain boundaries, which could also result in micro-cracking or lower hardness values as observed in case of sample sintered at 1500°C and 1600°C. A decrease of Vickers' hardness has been reported from the literature which gave the idea that conventionally sintered ZrB₂-B₄C ceramic base material showed lower hardness value due to the presence of residual stresses.

Higher densification value during spark plasma sintering due to formation of ZrC in the matrix as observed in XRD analysis observed in the material, which phenomena was not profound effect by analyzing XRD pattern in case of sample sintered at 1500°C and 1600°C.

Table 4.2: Relation between sintering temperature and hardness of sintered pellets

Sample	Sintering temperature (°C)	Vickers micro hardness(hv)
ZrB ₂ -B ₄ C-Mo ceramic matrix composite	1500	234
	1600	475
	1800	2788

4.5 Wear behavior of the sintered pellets:

While analysing wear behavior of ZrB₂-B₄C-Mo composites at different temperatures, graphical representation(Fig.4.13) showed that there is a drastic changes in material wear property while moving from conventional sintering to Spark Plasma Sintering (SPS).

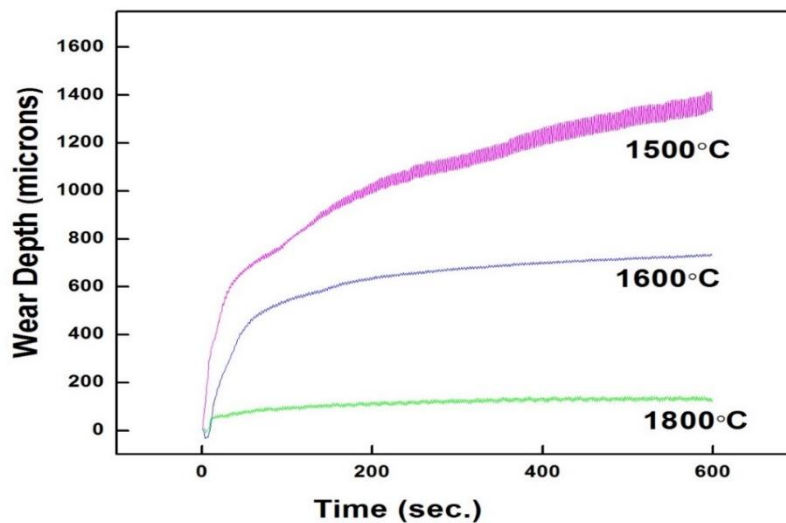


Fig 4.13: Variation of wear depth with sliding time for ZrB₂-B₄C-Mo composites for different sintering temperature.

It is cleared that the wear depth at 1500°C and 1600°C (in conventional sintering), was very much higher which are in the range of about 600-1400micron. But in spark plasma sintering, it was very much less (i.e. ~80micron). This may be due to liquid phase sintering Mo in the matrix during SPS and formation of ZrC and Mo₂BC which increases the hardness of the cermet as

confirmed from XRD and SEM analysis. As a result of which matrix became stronger, intergranular and intragranular region became densified resulting less wear of the matrix of the cermet. But this effect was not observed upto some extend in case of cermet sintered at 1500°C and 1600°C.

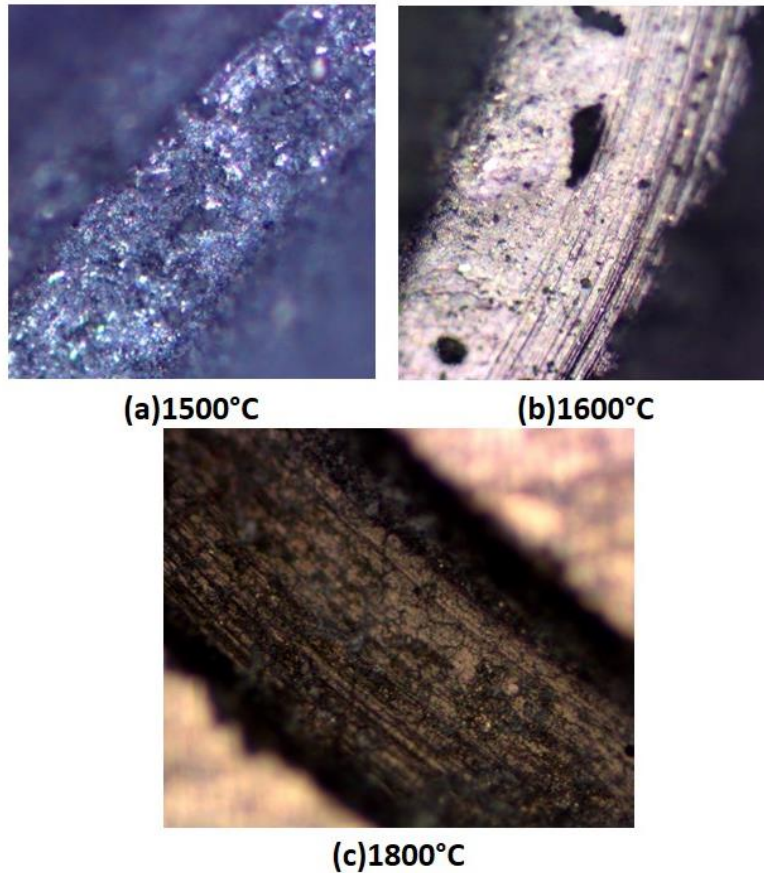


Fig 4.14: Optical microstructure of the worn surfaces of samples sintered at: (a) 1500°C, (b) 1600°C and (c) 1800°C, respectively.

The sample after wear test showed some micro-crack and porous behaviour in case of sintering at 1500°C and 1600°C (Fig4.14(a) and (b)). However such type of behaviour was found nominally in case of sample sintered at 1800°(Fig4.14 (c)). It is clear evident from the wear track thickness of sintered pellets at diiffrent tempertaures that the increases of sintering tempertaure wear track thickness is decreases this is due to the fact that at high tempertaure (1800°C) the hardness of the composite is maximum.

Chapter 5

Conclusions

5. Conclusions:

In the present study, considerable effort has been done to develop ZrB₂-B₄C-Mo composites by mechanical alloying and conventional sintering and spark plasma sintering to determine the degree of enhancement in mechanical properties will be presented with detailed characterization of the microstructural evolution. A major effort in this work has been devoted to explore the various routes of consolidation with variation of sintering temperatures for developing bulk components retaining the novel microstructure obtained by mechanical alloying.

By evaluating the results in terms of synthesis and characterization, consolidation, physical properties (density and porosity) and mechanical properties (hardness and wear resistant property) in all the composites with variation of process parameters, the conclusions are presented. The conclusions emerging from the results presented and discussed in this chapter may be summarized as:

- ❖ Mechanical alloying is a potential route for synthesis of ZrB₂-B₄C-Mo composites powders.
- ❖ XRD analysis of the milled product show that in each composite produces solid solution indicating that ZrB₂, B₄C, Mo dissolve in course of high-energy ball milling for 60 h.
- ❖ SEM analysis show the degree of size reduction of powders is the function of the milling time. The measurement of the average particle size of after 60 h of milling product show the reduction in particle size in the range of 5-10µm.
- ❖ SEM analysis of sintered pellets confirms that the presence of bright phase of ZrB₂ and dark phase of B₄C in the matrix.
- ❖ EDS analysis confirms the presence of elements Zr, B, C and Mo the results suggest that the final sintered products. It is clear that the bright phase showing the elemental peaks of Zr and B and dark phase contain the elemental peaks of B and C.

- ❖ Bulk physical properties (density and porosity) and mechanical properties (hardness and wear) for the present $\text{ZrB}_2\text{-B}_4\text{C-Mo}$ composites are the function of sintering temperatures.
- ❖ Composites sintered at 1800°C by spark plasma sintering shows superior mechanical properties (hardness and wear). It records the hardness value 27.34GPa (2788HV) as compared to the other composites sintered at lower temperature in conventional sintering technique.
- ❖ The ball-on-disc wear behavior of the present $\text{ZrB}_2\text{-B}_4\text{C-Mo}$ composites critically depends on the sintering temperature. The fretting wear data reveal that the wear volume, estimated principally from the transverse wear scar diameter, is the least in the sample sintered at 1800°C .

Thus, the above results suggest that mechanical alloying followed by conventional sintering and spark plasma sintering are a flexible, convenient and promising route for synthesizing $\text{ZrB}_2\text{-B}_4\text{C-Mo}$ composites with attractive mechanical properties. However, considering the entire spectrum of mechanical properties including hardness and wear, it is concluded that spark plasma sintering at 1800°C offers optimum combination of mechanical properties.

Reference:

- [1] Cutler RA. “Engineering properties of borides. In: Schneider SJ, editor. *Ceramics and glasses: engineered materials handbook*”, vol.4. Materials Park, OH: ASM International; 1991. p. 787–803.
- [2] Mroz C. Zirconium diboride. *Am Ceram Soc Bull* 1995; 76:164–5.
- [3] Upadhyaya K, Yang JM, Hoffman WP. “Materials for ultrahigh temperature structure applications”. *Am Ceram Soc Bull*, 1997; 58:51–6.
- [4] Norasetthekul S, Eubank PT, Bradley WL, Bozkurt B, Stucker B, “Use of zirconium diboride copper as an electrode in plasma applications”, *J Mater Sci* 1999;34:1261–70.
- [5] Levine SR, Opila EJ, Halbig MC, Kiser JD, Singh M, Salem JA. “Evaluation of ultra-high temperature ceramics for aero propulsion use”, *J Eur Ceram Soc* 2002; 22:2757–67.
- [6] Zhu S, Fahrenholtz WG, Hilmas GE. “Enhanced densification and mechanical properties of ZrB₂-SiC processed by a pre ceramic polymer coating route”, *Scripta Mater* 2008; 59:123–6.
- [7] Chamberlain AL, Fahrenholtz WG, Hilmas GE, Ellerby DT. “High-strength zirconium diboride-based ceramics”, *J Am Ceram Soc* 2004; 87(6):1170–2.
- [8] Monteverde F, Bellosi A. “Development and characterization of metal-diboride based composites toughened with ultra-fine SiC particulates”, *Solid State Sci* 2005; 5:622–30.
- [9] Wang HL, Wang CA, Yao XF, Fang DN. “Processing and mechanical properties of zirconium diboride-based ceramics prepared by spark plasma sintering”, *J Am Ceram Soc* 2007; 90:1992–7.

- [10] Zhang XH, Qu Q, Han JC, Han WB, Hong CQ. “Microstructural features and mechanical properties of ZrB₂-SiC-ZrC composites fabricated by hot pressing and reactive hot pressing”, *Scripta Mater*, 2008; 59:753–6.
- [11] Guo SQ, Kagawa Y, Nishimura T. “Mechanical behavior of two-step hot-pressed ZrB₂-based composites with ZrSi₂”, *J Eur Ceram Soc*, 2009;29(4):787–94.
- [12] Tian WB, Kan YM, Zhang GJ, Wang PL, “Effect of carbon nanotubes on the properties of ZrB₂-SiC ceramics”, *Mater Sci Eng A* 2008; 487:568–73.
- [13] Moya JS, Díaz M, Gutiérrez-González CF, Diaz LA, Torrecillas R, Bartolomé JF. Mullite-refractory metal (Mo, Nb) composites. *J Eur Ceram Soc* 2008;28:479–91.
- [14] Gu ML, Huang CZ, Zou B, Liu BQ, “Effect of (Ni, Mo) and TiN on the microstructure and mechanical properties of TiB₂ ceramic tool materials”, *Mater Sci Eng A* 2006; 433:39–44.
- [15] Deng Jianxin, Sun Junlong, “Microstructure and mechanical properties of hot-pressed B₄C/TiC/Mo ceramic composites,” *Ceramics International*, vol.35, pp.771–778, 2009.
- [16] XinYan Yue, ShuMao Zhao, Peng Lü, Qing Chang, HongQiang Ru, “Synthesis and properties of hot pressed B₄C–TiB₂ ceramic composite”, *Materials Science and Engineering A*, vol. 527, pp. 7215–7219, 2010.
- [17] I. Topcu, H.O. Gulsoy, N. Kadioglu, A.N. Gulluoglu, “Processing and mechanical properties of B₄C reinforced Al matrix composites,” *Journal of Alloys and Compounds*, vol.482, pp.516-521, 2009.
- [18] Han Wenbo, , Gao Jiaying, Zhang Jihong, Yu Jiliang, “Microstructure and Properties of B₄C-ZrB₂ Ceramic Composites” *International Journal of Engineering and Innovative Technology (IJEIT)*, vol 3, pp.163-166, 2013.

- [19] Choe H, Chen D, Schneibel JH. “Ambient to high temperature fracture toughness and fatigue-crack propagation behavior in a Mo-12Si-85B (at.%) Intermetallic”, *Intermetallic* 2001;9(4):319–29.
- [20] Bartolomé JF, Díaz M, Requena J, Moya JS, Tomsia AP. Mullite/molybdenum ceramic-metal composites. *Acta Mater* 1999; 47:3891–9.
- [21] Wang K, Robert RR. “The role of defects on thermophysical properties: thermal expansion of V, Nb, Ta, Mo and W”, *Mater Sci Eng R* 1998;23:101–37.
- [22] C. Suryanarayana, Nasser Al-Aqeeli “Mechanically alloyed Nano composites”, *Progress in Materials Science*, vol 58, 2013, pp 383–502.
- [23] Chawla KK, “Composite materials science and engineering”, 3rd ed. 2009, New York: Springer;.
- [24] Sumin Zhu, William G. Fahrenholtz, Gregory E. Hilmas, Shi C. Zhang, Edward J. Yadlowsky, Michael D. Keitz “Microwave sintering of a ZrB₂–B₄C particulate ceramic composite” *Composites volume 39* , 2008, pp 449–453
- [25] Hailong Wang, Deliang Chen, Chang-An Wang, Rui Zhang, Daining Fang ,” Preparation and characterization of high-toughness ZrB₂/Mo composites by hot-pressing process” *Int. Journal of Refractory Metals & Hard Materials*, vol 27 ,2009), pp 1024–1026
- [26] S.G. Huang*, K. Vanmeensel, J. Vleugels “Powder synthesis and densification of ultrafine B₄C–ZrB₂ composite by pulsed electrical current sintering” *Journal of the European Ceramic Society*, vol 34 , 2014, pp 1923–1933.

[27] Mahsa Jalal Mousavi, Mohammad Zakeri , Mohammad reza Rahimipour , Elham Amini “Mechanical properties of pressure-less sintered ZrB_2 with molybdenum, iron and carbon additives” Materials Science & Engineering vol 13, 2014, pp 3–7.

[28] R.V. Krishnaraon, Md.Zafir Alam, Dipak Kumar Das, V.V. Bhanu Prasad “Synthesis of ZrB_2 – SiC composite powder in air furnace” Ceramics International, vol 40, 2014, pp 15647–15653

[29] Mehdi Shahedi Asl, Mahdi Ghassemi Kakroudi, Behzad Nayebi “A fractographical approach to the sintering process in porous ZrB_2 – B_4C binary composites” Ceramics International, 2014.

[30] Caen Ang, Aaron Seeber, Kun Wang, Yi-Bing Cheng” Modification of ZrB_2 powders by a sol–gel ZrC precursor—A new approach for ultra-high temperature ceramic composites” Journal of Asian Ceramic Societies, vol-1, 2013, pp 77–85